

# REPORT DOCUMENTATION PAGE

Form Approved  
OMB NO. 0704-0188

Public Reporting burden for this collection of information is estimated to average 1 hour per response, including the time for reviewing instructions, searching existing data sources, gathering and maintaining the data needed, and completing and reviewing the collection of information. Send comment regarding this burden estimates or any other aspect of this collection of information, including suggestions for reducing this burden, to Washington Headquarters Services, Directorate for Information Operations and Reports, 1215 Jefferson Davis Highway, Suite 1204, Arlington, VA 22202-4302, and to the Office of Management and Budget, Paperwork Reduction Project (0704-0188) Washington, DC 20503.

1. AGENCY USE ONLY (Leave Blank)		2. REPORT DATE	3. REPORT TYPE AND DATES COVERED  Technical 04/15/1997 to 10/14/2000	
4. TITLE AND SUBTITLE  Joint Services Optics Program Research in the Optical Sciences		5. FUNDING NUMBERS  DAAG55-97-1-0116		
6. AUTHOR(S)  James C. Wyant				
7. PERFORMING ORGANIZATION NAME(S) AND ADDRESS(ES)  University of Arizona Optical Sciences Center 1630 E. University Blvd. Tucson AZ 85721		8. PERFORMING ORGANIZATION REPORT NUMBER  None		
9. SPONSORING / MONITORING AGENCY NAME(S) AND ADDRESS(ES)  U. S. Army Research Office P.O. Box 12211 Research Triangle Park, NC 27709-2211		10. SPONSORING / MONITORING AGENCY REPORT NUMBER  ARO 36175.1 - PH		
11. SUPPLEMENTARY NOTES  The views, opinions and/or findings contained in this report are those of the author(s) and should not be construed as an official Department of the Army position, policy or decision, unless so designated by other documentation.				
12 a. DISTRIBUTION / AVAILABILITY STATEMENT  Approved for public release; distribution unlimited.		12 b. DISTRIBUTION CODE		
13. ABSTRACT (Maximum 200 words)  This report describes research on eight different projects ranging from fundamental quantum optics to optical engineering. Topics discussed include the following: Study of magnetoexciton femtosecond spectroscopy, semiconductor microcavities, and periodic structures, ion trapping and quantum transport in optical lattices, quantum atom optics, design optimization of circular grating DBR lasers, coherent and incoherent ultrafast nonlinear optical processes in anisotropically strained semiconductor quantum wells, portable MWIR computed tomography imaging spectroscopy, and the numerical modeling of nonlinear optical frequency conversion. The JSOP program supported more than 25 graduate students and resulted in more than 115 publications and 4 patent disclosures. Some of the projects involved interactions with colleagues and DOD laboratories such as the Army Research Labs and Redstone Arsenal. University/industry interactions on these projects occurred through direct collaboration with colleagues at several companies including Raytheon and Motorola and through participation in the Center for Optoelectronic Devices, Interconnects and Packaging.				
14. SUBJECT TERMS  Semiconductor Microcavities, Femtosecond Spectroscopy, Atom Optics, Semiconductor Quantum Wells, DBR Lasers, Optical Lattices, Imaging Spectrometer			15. NUMBER OF PAGES  50	16. PRICE CODE
17. SECURITY CLASSIFICATION OR REPORT UNCLASSIFIED	18. SECURITY CLASSIFICATION ON THIS PAGE UNCLASSIFIED	19. SECURITY CLASSIFICATION OF ABSTRACT UNCLASSIFIED	20. LIMITATION OF ABSTRACT UL	

NSN 7540-01-280-5500

Standard Form 298 (Rev.2-89)  
Prescribed by ANSI Std. Z39-18  
298-102

20010116 127

**CONTENTS**

<b>Magnetoexciton Femtosecond Spectroscopy.....</b>	1
H. Gibbs	
<b>Semiconductor Microcavities and Periodic Structures.....</b>	6
G. Khitrova	
<b>Atom Trapping and Quantum Transport in Optical Lattices.....</b>	12
P. Jessen	
<b>Collective Effects in Atom Optics.....</b>	17
P. Meystre	
<b>Design Optimization of Circular Grating DBR Lasers for High Power</b>	
<b>Applications.....</b>	25
M. Fallahi	
<b>Coherent and Incoherent Ultrafast Nonlinear Optical Processes in Anisotropically Strained</b>	
<b>Semiconductor Quantum Wells.....</b>	30
R. Binder	
<b>Portable MWIR Computed Tomography Imaging Spectrometer (CTIS).....</b>	36
M. Descour	
<b>Numrical Modeling of Nonlinear Optical Frequency Conversion.....</b>	45
R. Eckardt	

# MAGNETOEXCITON FEMTOSECOND SPECTROSCOPY

Hyatt M. Gibbs

## *Statement of the Problem Studied*

Femtosecond spectroscopy was performed on InGaAs/GaAs quantum wells with very narrow absorption linewidths both bare and in a microcavity in order to study higher order carrier-carrier and field-carrier correlations.

## *Summary of the Most Important Results*

There have been many pump-probe experiments on semiconductor quantum wells (QW's) in the last two decades. Nonetheless, the results and interpretations are controversial. Part of the reason for these controversies is the difficulty of obtaining samples with very narrow exciton linewidths that can be studied in transmission. Removal of the substrate, essential for GaAs/AlGaAs QW's, usually broadens the lines observed in reflection before the removal. Our very narrow-linewidth InGaAs/GaAs QW's on GaAs substrates that are transparent at the QW exciton transition are ideal for such studies. We pump the exciton resonance of such samples resonantly or near resonantly and probe all of the surrounding wavelengths to ascertain the relative contributions of screening, state filling, broadening, and the AC Stark shift. The original proposal used magnetic field studies as the unifying theme. As the research progressed, the study of higher order carrier-carrier and field-carrier correlations became the unifying theme. This was due to the difficulty of optical access in our solenoidal superconducting magnet, the difficulty of computing the relevant dynamics in the presence of a magnetic field, and the unexpected richness of the zero-field data.

Differential absorption spectra of high-quality InGaAs quantum wells were obtained for various pump detunings and polarization configurations. For low intensity pump pulses tuned well below the exciton, a *redshift* was observed for oppositely circularly polarized pump and probe pulses. Microscopic calculations in the  $\chi^{(3)}$  limit show that this redshift originates from both, memory effects in the Coulomb-induced excitonic correlations and the bound two-exciton state. This discovery was especially important because the leading term is a four-particle correlation, i.e. the signal is background free provided the light-hole resonance is far away. Such is not the case for GaAs/AlGaAs quantum wells, explaining why this redshift was not seen before. The redshift is 20% as large as the usual blue shift for co-circularly polarized pump and probe pulses, so it is not a small effect. One can think of the effect as a correlation between the pump-induced excitonic polarization and the probe-induced excitonic polarization; these would be independent and uncorrelated were it not for the Coulomb interaction. [Sieh et al. 1999]

These studies were pursued to higher intensities, revealing features attributed to  $\chi^{(5)}$  effects. For resonant excitation with increasing pump intensity a saturation of both the exciton bleaching and the induced absorption due to two-exciton resonances is observed, whereas for pumping below the exciton a characteristic polarization dependence of higher-order contributions to the optical Stark effect is found. Microscopic calculations including Coulomb correlations show that the experimental observations can be described by the coherent dynamics of single- and two-exciton resonances up to fifth order in the optical field. [Meier et al. 2000]

The  $\chi^{(3)}$  and  $\chi^{(5)}$  experiments were performed on 30 quantum wells with periodicities far from the  $\lambda_x/2$  Bragg condition to minimize radiative coupling effects. An experiment was performed on a sample with 100 quantum wells with periods scanned through the Bragg condition in order to study the effect of a magnetic-field increase in the exciton oscillator strength on the radiative coupling. Measurements were made of the time-integrated photoluminescence in magnetic fields of up to 10 T as a function of the detuning from the Bragg resonance. At  $B = 0$  the Bragg condition is characterized by a lack of emission, while the radiative exciton coupling shows up as a large radiative mode splitting at detunings close to Bragg. As  $B$  increases, the whole mode structure shifts to higher photon energies due to the diamagnetic shift of the  $n=1$  hh exciton in the magnetic field. In addition, the **magnetic field causes the mode splitting near the Bragg resonance to increase**, as expected for an increase of oscillator strength. The percentage increase of the splitting saturates for magnetic fields higher than  $B = 5$  T and reaches about 30% for the  $\sigma^+$  component and 20% for  $\sigma^-$ . The same qualitative behavior is observed for the modes on the other side of the Bragg resonance. A saturation of the increase in oscillator strength was observed for magnetic fields larger than 6 T and attributed to heavy-hole light-hole mixing and possible strain effects. The larger final splitting observed for the  $\sigma^+$  component of the PL is most likely due to the paramagnetic splitting that occurs between the two polarizations in the QW. [Spiegelberg et al. 2000]

We have grown and studied normal-mode-coupling microcavities containing one or two QW's and exhibiting record splitting to linewidth ratios for some time [Khitrova et al. 1999]. Lee and Norris performed coherent control experiments on one of our samples, seeking to control a signal pulse at the upper-branch transmission peak with a pair of control pulses at the lower-branch transmission peak. Indeed they found quite good control, but with an inevitable small component that decays slowly [Lee et al. 1998]. More significantly from a semiconductor physics point of view was the observation of some oscillations in the measured differential reflectivity as a function of probe delay with respect to the first excitation pulse. The oscillations had a period of 2 ps independent of the pump fluence and consistent with the energy difference between the excitonic resonance and the upper normal mode. The oscillations are strongly enhanced when the phase between the two pump pulses is  $-130^\circ$ . The fact that the oscillations persisted for several ps suggested that they might arise from intraband coherences that live longer than the interband polarization that dies in less than 1 ps for their experiment. In parallel Kira, Jahnke, and Koch were developing a fully quantized theory of the optical interactions with semiconductors that revealed quantum correlations between the field and carrier density. As a happy coincidence between experimental and theoretical advances, the theorists found that these **quantum correlations lead to intraband coherences which live much longer than the interband dephasing time and can be observed as oscillations in the time-resolved reflectivity from a normal-mode microcavity**. Even the detailed phase dependence is well reproduced by the theory [Lee et al. 1999]. Another manifestation of field-carrier intraband correlations is the appearance of a third transmission peak for single-beam or pump-probe transmission through a normal-mode microcavity while the usual two peaks persist [Ell et al. 2000].

### ***List of Publications and Technical Reports***

1. Belousov, M. V., A. Yu. Chernyshov, I. V. Ignatev, I. E. Kozin, A. V. Kavokin, H. M. Gibbs, and G. Khitrova, "Statistical Model Explaining the Fine Structure and Interface Preference of Localized Excitons in Type-II GaAs/AlAs Superlattices," *J. Nonlinear Opt. Phys. Matls.* **7**, 13 (1998).
2. Brick, P., C. Ell, M. Hübner, J. Prineas, G. Khitrova, H. M. Gibbs, C. Sieh, T. Meier, F. Jahnke, A. Knorr, and S. W. Koch, "Coulomb memory effects and higher order Coulomb correlations in the excitonic optical Stark effect," *Phys. Status Solidi A* **178**, 459 (2000).
3. Brick, P., O. Lyngnes, C. Ell, M. Hübner, E. S. Lee, G. Khitrova, H. Gibbs, M. Kira, F. Jahnke, and S. W. Koch, "Signatures of quantum correlations in a semiconductor microcavity," *Phys. Status Solidi B* **221**, 107 (2000).
4. Brick, P., C. Ell, G. Khitrova, H. M. Gibbs, T. Meier, S. W. Koch, " $\chi^{(5)}$ -signatures in the optical Stark effect," QTuI4, Quantum Electronics and Laser Science Conference, San Francisco, May 7-12, 2000.
5. Ell, C., P. Brick, M. Hübner, E. S. Lee, O. Lyngnes, J. P. Prineas, G. Khitrova, H. M. Gibbs, M. Kira, F. Jahnke, S. W. Koch, D. G. Deppe, and D. L. Huffaker, "Quantum correlations in the nonperturbative regime of semiconductor microcavities," *Phys. Rev. Lett.*, to be published (2000).
6. Gibbs, H. M., C. Ell, G. Khitrova, J. Prineas, T.R. Nelson, Jr., S. Park, E. Lee, R. Houdré, S.W. Koch, "Linewidths of normal-mode-coupling microcavities", RWD1, Workshop on Radiative Processes and Dephasing in Semiconductors, Coeur d'Alene, Idaho, February 2-4, 1998.
7. Gibbs H. M., G. Khitrova, J. D. Berger, D. V. Wick, T. R. Nelson, Jr., S. W. Koch, M. Kira, and F. Jahnke, "Photoluminescence from a normal-mode-coupling semiconductor microcavity," QTuA3, International Quantum Electronic Conference (IQEC'98), San Francisco, May, 3-8, 1998.
8. Gibbs, H. M., "VCSEL History Shows Value of Fundamental Research", *Laser Focus World*, August, 1999.
9. Khitrova, G., H. M. Gibbs, F. Jahnke, M. Kira, and S. W. Koch, "Nonlinear optics of normal-mode coupling semiconductor microcavities," *Rev. Mod. Phys.* **71**, 1591-1640 (1999).
10. Koch, S. W., C. Sieh, T. Meier, F. Jahnke, A. Knorr, P. Brick, M. Hübner, C. Ell, J. Prineas, G. Khitrova, and H. M. Gibbs, "Theory of coherent effects in semiconductors," *J. Lumin.* **83-84**, 1 (1999).

11. Lee, Y.-S., A. Maslov, T. B. Norris, D. S. Citrin, J. Prineas, G. Khitrova, and H. M. Gibbs, "Coherent control of normal modes in quantum-well semiconductor microcavity," International Quantum Electronic Conference (IQEC'98 post-deadline QPD2), San Francisco, May, 3-8, 1998.
12. Lee, Y.-S., T. B. Norris, A. Maslov, D. S. Citrin, J. Prineas, G. Khitrova, and H. M. Gibbs, "Coherent control of polaritons in a quantum well microcavity," QMF1, Quantum Electronics and Laser Science Conference, Baltimore, May 23-28, 1999.
13. Lee, Y.-S., T. B. Norris, M. Kira, S. W. Koch, A. Maslov, D. S. Citrin, G. Khitrova, and H. M. Gibbs, "Correlations and coherent control of normal modes in a microcavity," *Phys. Status Solidi A* **178**, 391 (2000).
14. Lee, Y.-S., T. B. Norris, M. Kira, F. Jahnke, S. W. Koch, G. Khitrova, and H. M. Gibbs, "Quantum correlations and intraband coherences in semiconductor cavity QED," *Phys. Rev. Lett.* **83**, 5338 (1999).
15. Lee, Y.-S., T. B. Norris, J. Prineas, G. Khitrova, and H. M. Gibbs, "Nondegenerate coherent control of polariton modes in a quantum-well semiconductor microcavity," *Phys. Status Solidi B* **221**, 121 (2000)
16. Lee, Y.-S., T. B. Norris, M. Kira, F. Jahnke, S. W. Koch, G. Khitrova, and H. M. Gibbs, "Quantum correlation induced intraband coherences in a quantum-well microcavity," QTuB6, Quantum Electronics and Laser Science Conference, San Francisco, May 7-12, 2000.
17. Meier, T., C. Sieh, S. W. Koch, P. Brick, M. Hübner, C. Ell, J. Prineas, G. Khitrova, and H. M. Gibbs, "Influence of carrier-correlations on the optical Stark effect of semiconductors," QMC6, Quantum Electronics and Laser Science Conference, Baltimore, May 23-28, 1999.
18. Meier, T., S. W. Koch, P. Brick, C. Ell, G. Khitrova, and H. M. Gibbs, "Signatures of correlations in intensity-dependent excitonic absorption changes," *Phys. Rev. B* **62**, 4218 (2000).
19. Norris, T. B., Y.-S. Lee, M. Kira, F. Jahnke, S. W. Koch, G. Khitrova, and H. M. Gibbs, "Coherent control and quantum correlations in semiconductor microcavities," SPIE Photonic West, *Ultrafast Phenomena in Semiconductors IV*, San Jose, January 27, 2000. Invited.
20. Rühle, W. W., S. Hallstein, J. D. Berger, M. Hilpert, H. C. Schneider, F. Jahnke, S. W. Koch, H. M. Gibbs, G. Khitrova, and M. Oestreich, "Pulsed vertical-cavity-laser emission synchronized to electron spin precession," *Phys. Status Solidi B* **206**, 387 (1998).

21. Sieh, C., T. Meier, F. Jahnke, A. Knorr, S. W. Koch, P. Brick, M. Hübner, C. Ell, J. Prineas, G. Khitrova, and H. M. Gibbs, "Coulomb memory signatures in the excitonic optical Stark effect," *Phys. Rev. Lett.* **82**, 3112 (1999).
22. Spiegelberg, C., H. M. Gibbs, J. Prineas, C. Ell, P. Brick, E. S. Lee, G. Khitrova, V. V. Zapasskii, M. Hübner, and S. W. Koch, "Photoluminescence and pump-probe spectroscopy of Bragg and off-Bragg quantum wells", *Phys. Status Solidi B* **221**, 85 (2000).

### ***Scientific Personnel***

#### Graduate Students partially supported by this grant

Sahnggi Park, Ph.D. December 1999  
John Prineas, Ph.D. May 2000

#### Research Associate

Martin Huebner

#### Assistant Research Professor

Christine Spiegelberg

#### Professors

Hyatt M. Gibbs  
Stephan Koch  
Galina Khitrova

#### ***Report of Inventions***

None

#### ***Technology Transfer***

Transfer of technology is through publications and discussions with Dr. George Simonis, Army Research Labs, and Dr. Charles Bowden, Redstone Arsenal, at various meetings and with member company representatives twice a year at the meetings of the Center for Optoelectronic Devices, Interconnects and Packaging. I participated in the Workshop on Nanostructures for DoD Applications organized by Henry Everitt and held at Georgia Tech in October; we had multiple discussions with both army and air force personnel.

## SEMICONDUCTOR MICROCAVITIES AND PERIODIC STRUCTURES

Galina Khitrova

### *Statement of the Problem Studied*

This project focused on the radiative coupling between quantum-well excitonic resonances and the optical field in semiconductor microcavities exhibiting normal-mode coupling (NMC) or in a periodic array of multiple quantum wells (MQW's).

### *Summary of the Most Important Results*

#### **Radiative Coupling Between Quantum Wells Can Dominate the Total Linewidth and Determine the Spectra of Photoluminescence and Secondary Emission**

When thin quantum wells are spaced apart by half the heavy-hole-exciton wavelength  $\lambda_x$  in the material (Bragg condition), radiative coupling effects are especially pronounced because of the constructive interference between all of the quantum wells. The effects are larger the narrower the exciton linewidth and they are easier to interpret if the light-hole transition is far removed. Both advantages occur in our InGaAs/GaAs periodic quantum well samples that we have grown by MBE with numbers of quantum wells  $N = 1, 10, 30, 60, 100$ , and 200. That radiative coupling between quantum wells could be very important was first shown theoretically by Ivchenko and experimentally by Kochereshko et al., and by several other groups.

Our principal contributions are the following. We extracted the radiative linewidth from a plot of the measured total Bragg-condition linewidth in reflectivity versus the number of quantum wells (QW's)  $N$ . This also showed that the radiative linewidth of the coupled quantum wells' superradiant mode could exceed the inhomogeneous linewidth by more than an order of magnitude. We showed much more clearly than before that the  $N$  normal modes associated with  $N$  quantum wells cluster energetically around two branches giving rise to a splitting of the true absorption  $A = 1 - R - T$  when the period  $d$  is different from  $\lambda_x/2$ . The "superradiant" mode has several curious features. The reflectivity  $R$  is broadest and strongest at  $d = \lambda_x/2$ ; this means that it is difficult for light to go into a  $d = \lambda_x/2$  structure. The measured  $R$  and transmission  $T$  are largest and  $A$  is smallest when  $d = \lambda_x/2$  is satisfied. Transfer matrix computations show that for  $d = \lambda_x/2$ , the standing wave of light has minima at the position of each of the QW's; this is forced by the QW refractive index. This is completely different from the case of a microcavity, where the mirrors determine the field peak positions and a QW can be placed anywhere within the standing wave. Away from  $d = \lambda_x/2$ , it is impossible to have a node at every QW in the periodic structure; consequently the absorption must increase, as we observe.

Even more importantly, we showed that the normal-mode splitting discussed above for  $A$  is even seen in photoluminescence following excitation into the electron-hole continuum. The photoluminescence intensity emitted normally goes through a minimum as the period is scanned through the Bragg condition, the emission occurring preferentially at off-Bragg nonzero angles; i.e., the "superradiant" mode emission is suppressed. The photoluminescence clearly exhibits polaritonic features in that the spectrum away from  $d = \lambda_x/2$  is double peaked much like the

computed energies. This is entirely different from  $N$  times the measured single QW photoluminescence spectrum which is single peaked with a width that decreases to the measured absorption width as the excitation density is reduced to zero. Clearly radiative coupling effects, not the single QW emission spectrum, determine the coupled Bragg quantum well spectra.

We found that the radiative coupling for  $N = 100$  is so strong that it dominates all of the emission's spectral and angular properties for not only incoherent photoluminescence [Hübner, Prineas, et al. 1999] but also coherent resonance Rayleigh scattering (coherent secondary emission) [Prineas et al. 2000]. As quantum well linewidths become narrower and narrower such radiative coupling effects will dominate the system's optical properties for all periods, making them quite different from what would be expected from the susceptibility of a single quantum well.

### **Vacuum-Field Rabi Splitting in Planar and 3D Microcavities**

In our planar semiconductor microcavities all the linear features can be understood well by using a linear dispersion theory. In the linear dispersion theory, the light field is treated classically, i.e., by solving Maxwell's wave equation taking the boundary conditions at each interface of the semiconductor microcavity structure into account. The response of the material, the susceptibility, enters the wave equation via the polarization. It can be determined by measuring the excitonic absorption coefficient and calculating the corresponding refractive index via the Kramers-Kronig relation. Or, it can be calculated based on a microscopic theory. It has been successfully applied to understand the semiconductor NMC linewidths. The NMC linewidths are determined by the absorption and refractive index in the immediate vicinity of the NMC peaks. Since the NMC transmission is determined by the absorption at each NMC peak, the exciton lineshape asymmetry (from structural disorder or nonlinear effects) results in unequal transmission peaks for zero cavity-exciton detuning [Ell et al. 1998].

The sensitivity of the NMC transmission and linewidth to local absorption is quite apparent in nonlinear studies. We have measured the nonlinear transmission and reflection of our NMC microcavities both by pump/probe and by femtosecond reflection and upconversion [Khitrova et al. 1999]. Because of our narrow quantum-well linewidth, we saw a new nonlinear behavior: the transmission drops to zero with almost no reduction in NMC splitting. This behavior can be explained well by nonlinear dispersion theory using the measured exciton absorption with increased electron-hole density in the transfer matrix formalism. The exciton broadens before it loses oscillator strength. As the exciton broadens, the absorption increases at the detuned wavelength of the NMC transmission peaks, thus decreasing the Fabry-Pérot transmission. Since the area under the exciton absorption, i.e. the oscillator strength, changes very little as the broadening sets in, there is almost no reduction in splitting while the transmission drops to zero. This nonlinear behavior is also in good agreement with calculations based on a microscopic theory. Other groups failed to see this curious nonlinear behavior because the inhomogeneous broadening in their quantum wells masked the exciton broadening. Again, this illustrates the importance of understanding the quantum well susceptibility well if one is to understand the coupled system.

That our microcavities operate semiclassically can be seen from two facts. First, we can understand their nonlinear behavior within a semiclassical theory. And, second, we measure that  $2 \times 10^5$  photons must be absorbed from a 150-fs pulse in a 50- $\mu\text{m}$ -diameter beam to drop the peak absorption coefficient in half [Khitrova et al. 1999]. The latter causes the NMC transmission to drop to 15 to 20%. Thus, present-day planar semiconductor microcavities operate much like the many-atom case. It is the very large quantum-well absorption coefficient, i.e. the potential for exciton formation, which gives rise to the observed NMC splitting. In order to see true VRS, i.e. true quantum effects, one has to [Ell, Gibbs, et al. 1999] reduce (i) the cavity mode volume and (ii) go from a quantum well to a quantum dot. Extrapolating from  $\approx 10^5$  to  $\approx 1$  suggests that a large quantum dot of a diameter of 158 nm might be sufficiently small to exhibit the required quantum effects.

### *List of Publications and Technical Reports*

1. Ammerlahn, D., J. Kuhl, B. Grote, S. W. Koch, G. Khitrova, H. Gibbs, R. Hey, and K. H. Ploog, "Radiative coupling in single quantum wells and Bragg structures," *Phys. Status Solidi B* **221**, 101 (2000).
2. Binder, R., M. Lindberg, A. Schülzgen, M. E. Donovan, K. Wundke, H. M. Gibbs, G. Khitrova, and N. Peyghambarian, "Many-body aspects of excitonic Rabi oscillations in semiconductors," SPIE Photonics West 99, San Jose. Invited.
3. Ell, C., J. Prineas, T. R. Nelson, Jr., S. Park, H. M. Gibbs, G. Khitrova, S. W. Koch, and R. Houdré, "Influence of structural disorder and light coupling on the excitonic response of semiconductor microcavities," *Phys. Rev. Lett.* **80**, 4795 (1998).
4. Ell, C., J. Prineas, T. R. Nelson, Jr., S. Park, H. M. Gibbs, G. Khitrova, S. W. Koch, R. Houdré, "Disorder-averaged excitonic response and its application to normal-mode coupling in semiconductor microcavities within a linear dispersion theory", QTUG2, International Quantum Electronic Conference (IQEC'98), San Francisco, May, 3-8, 1998.
5. Ell, C., M. Hübner, J. P. Prineas, P. Brick, E. S. Lee, G. Khitrova, and H. M. Gibbs, "Normal mode coupling in optical lattices of excitons in periodic quantum well structures," *Optics and Photonic News* **10** (12), 25 (1999).
6. Ell, C., J. Prineas, T. R. Nelson, Jr., S. Park, E. S. Lee, H. M. Gibbs, G. Khitrova, and S. W. Koch, "Excitonic Features in Semiconductor Microcavities", in "Advances in Laser Physics", eds. V. S. Letokhov and P. Meystre, p. 67, Harwood Academic Publishers, Malaysia 2000.
7. Ell, C., H. M. Gibbs, G. Khitrova, E. S. Lee, S. Park, D. G. Deppe, and D. L. Huffaker, "Toward quantum entanglement in a quantum-dot nanocavity," 1999 IEEE/LEOS Summer Topical Meetings, VCSELs and Microcavities, 28-30 July 1999, San Diego. LEOS Newsletter **13** (4), 8 (1999).

8. Ell, C., J. P. Prineas, P. Brick, M. Hübner, H. M. Gibbs, G. Khitrova, S. W. Koch, "Linear and nonlinear optical properties of Bragg and off-Bragg periodic quantum well structures," QWA4, Quantum Electronics and Laser Science Conference, San Francisco, May 7-12, 2000.
9. Hübner, M., J. Kuhl, B. Grote, T. Stroucken, S. Haas, A. Knorr, S. W. Koch, G. Khitrova, H. Gibbs, "Influence of superradiant exciton/photon coupling on the nonlinear optical response in a wedged quantum well Bragg structure", RTuA4, Workshop on Radiative Processes and Dephasing in Semiconductors, Coeur d' Alene, February 2-4, 1998.
10. Hübner, M., J. Kuhl, B. Grote, T. Stroucken, S. Haas, A. Knorr, S. W. Koch, G. Khitrova, and H. M. Gibbs, "Superradiant coupling of excitons in (InGa)As multiple quantum wells," *Phys. Status Solidi B* **206**, 333 (1998).
11. Hübner, M., J. P. Prineas, C. Ell, P. Brick, E. S. Lee, G. Khitrova, H. M. Gibbs, and S. W. Koch, "Optical lattices achieved by excitons in periodic quantum structures," *Phys. Rev. Lett.* **83**, 2841 (1999).
12. Hübner, M., C. Ell, P. Brick, J. Prineas, G. Khitrova, H. M. Gibbs, W. Hoyer, M. Kira, and S. W. Koch, "Emission from Radiatively Coupled Periodic Quantum Well Structures", *Adv. Solid State Phys.* **39**, 443 (1999).
13. Hübner, M., C. Ell, J. Prineas, P. Brick, E. S. Lee, G. Khitrova, H. M. Gibbs, W. Hoyer, M. Kira, and S. W. Koch, "Signatures of polaritonic normal modes in the photoluminescence from periodic quantum well structures following continuum excitation," QMF4, Quantum Electronics and Laser Science Conference, Baltimore, May 23-28, 1999.
14. Khitrova, G., D. V. Wick, J. D. Berger, C. Ell, J. P. Prineas, T. R. Nelson, Jr., O. Lyngnes, H. M. Gibbs, M. Kira, F. Jahnke, S. W. Koch, W. Rühle, and S. Hallstein, "Excitonic effects, luminescence, and lasing in semiconductor microcavities," *Phys. Status Solidi B* **206**, 3 (1998).
15. Khitrova, G., H. M. Gibbs, F. Jahnke, M. Kira, and S. W. Koch, "Nonlinear optics of normal-mode coupling semiconductor microcavities," *Rev. Mod. Phys.* **71**, 1591-1640 (1999).
16. Kira, M., F. Jahnke, S. W. Koch, J. D. Berger, D. V. Wick, T. R. Nelson, Jr., G. Khitrova, and H. M. Gibbs, "Quantum Theory of Spontaneous Emission from Microcavities," *SPIE 3283*, 212 (1998).
17. Kira, M., F. Jahnke, S. W. Koch, T. R. Nelson, Jr., D. V. Wick, G. Khitrova, and H. M. Gibbs, "Quantum theory of semiconductor microcavities," RWB5, Workshop on Radiative Processes and Dephasing in Semiconductors, Coeur d' Alene, February 2-4, 1998.

18. Kuhl, J., M. Hübner, D. Ammerlahn, G. Grote, T. Stroucken, S. Haas, A. Knorr, S.W. Koch, G. Khitrova, H.M. Gibbs, R. Hey, K. Ploog, "Coherent dynamics of coupled exciton-photon modes in multiple quantum wells and microcavities", QFB1, International Quantum Electronic Conference (IQEC'98), San Francisco, May 3-8, 1998.
19. Kuhl, J., M. Hübner, D. Ammerlahn, T. Stroucken, B. Grote, S. Haas, S. W. Koch, G. Khitrova, H. Gibbs, R. Hey, and K. Ploog, "Coherent dynamics of excitons in radiatively coupled quantum well structures and microcavities," FB2, Nonlinear Optics '98, Princeville, Kauai, Hawaii, August 10-14, 1998.
20. Kuhl, J., M. Hübner, D. Ammerlahn, T. Stroucken, B. Grote, S. Haas, S. W. Koch, G. Khitrova, H. M. Gibbs, R. Hey, and K. Ploog, "Superradiant exciton/light coupling in semiconductor heterostructures – II: Experiments," *Adv. Solid State Physics* **38**, 281 (1998).
21. Lee, E. S., S. Park, C. Ell, P. Brick, H. M. Gibbs, and G. Khitrova, D. G. Deppe, and D. L. Huffaker, "Normal mode coupling in a 3D semiconductor nanocavity," QTuA20 Quantum Electronics and Laser Science Conference, San Francisco, May 7-12, 2000.
22. Lee, Y.-S., T. B. Norris, M. Kira, F. Jahnke, S. W. Koch, G. Khitrova, and H. M. Gibbs, "Coherent control of cavity-polariton secondary emission," QThQ4 Quantum Electronics and Laser Science Conference, San Francisco, May 7-12, 2000.
23. Park, S., V. Zapasskii, D. V. Wick, T. R. Nelson, Jr., C. Ell, H. M. Gibbs, G. Khitrova, A. Schülzgen, M. Kira, F. Jahnke, and S. W. Koch, "Spontaneous emission lifetime of carriers in a semiconductor microcavity measured by photoluminescence without distortion by reabsorption", *Optics Express* **4**, 512 (1999).
24. Prineas, J. P., E. S. Lee, C. Ell, H. M. Gibbs, G. Khitrova, "Linear spectral of radiatively coupled excitons in InGaAs quantum well structures", QFB7, International Quantum Electronic Conference (IQEC'98), San Francisco, May, 3-8, 1998.
25. Prineas, J. P., C. Ell, E. S. Lee, G. Khitrova, H. M. Gibbs, "Identification of individual normal modes of light-coupled semiconductor quantum wells in linear spectra," *Phys. Status Solidi A* **178**, 455 (2000).
26. Prineas, J. P., C. Ell, E. S. Lee, G. Khitrova, H. M. Gibbs, and S. W. Koch, "Exciton-polariton eigenmodes in light-coupled  $In_{0.04}Ga_{0.96}As/GaAs$  semiconductor multiple-quantum-well periodic structures" *Phys. Rev. B* **61**, 13863 (2000).
27. Prineas, J. P., J. Shah, B. Grote, C. Ell, G. Khitrova, H. M. Gibbs, and S. W. Koch, "Dominance of Radiative Coupling over Disorder in Resonance Rayleigh Scattering in Semiconductor Multiple Quantum-Well Structures", *Phys. Rev. Lett.* **85**, 3041 (2000).
28. Schülzgen, A., R. Binder, M. E. Donovan, M. Lindberg, K. Wundke, H. M. Gibbs, G. Khitrova, and N. Peyghambarian, "Direct observation of excitonic Rabi oscillations in semiconductors," *Phys. Rev. Lett.* **82**, 2346 (1999).

29. Schülzgen, A., R. Binder, M. E. Donovan, K. Wundke, H. M. Gibbs, G. Khitrova, N. Peyghambarian, M. Lindberg, "Excitonic Rabi oscillations in semiconductors," *Optics and Photonic News* 10 (12), 39 (1999).
30. Schülzgen, A., R. Binder, M. E. Donovan, K. Wundke, H. M. Gibbs, G. Khitrova, N. Peyghambarian, and M. Lindberg, "Laser-induced Rabi oscillations in semiconductors," QMC5, Quantum Electronics and Laser Science Conference, Baltimore, May 23-28, 1999. Invited.

***Scientific Personnel***

**Graduate Students partially supported by this grant**

Tom Nelson, Ph. D., January 1998  
Eun Seong Lee  
John Prineas, Ph. D., May 2000

**Associate Research Professor**

Claudia Ell

**Professors**

Galina Khitrova  
Stephan Koch  
Hyatt Gibbs

***Report of Inventions***

None

***Technology Transfer***

Discussions with Dr. George Simonis, Army Research Labs, and Drs. Charles Bowden and Jonathon Dowling, Redstone Arsenal, at various meetings along with publications constitute the technology transfer for this project. I participated in the Workshop on Nanostructures for DoD Applications organized by Henry Everitt and held at Georgia Tech in October 1998; we had multiple discussions with both Army and Air Force personnel.

## ATOM TRAPPING AND QUANTUM TRANSPORT IN OPTICAL LATTICES

Poul S. Jessen

### *Statement of the Problem Studied*

The focus of our work during the grant period has been to develop neutral Cesium atoms trapped in far-off-resonance optical lattices into a powerful model system for the exploration of quantum control, quantum transport and quantum coherent dynamics. At the outset our major goals were:

- (i) To demonstrate efficient loading and trapping of Cs atoms in optical lattices formed by light detuned a few thousand linewidths from atomic resonance.
- (ii) To develop and experimentally demonstrate a new scheme for resolved sideband Raman cooling, in order to prepare atoms in the vibrational ground state of individual potential wells in a far-off-resonance optical lattice.
- (iii) To study quantum transport and mesoscopic quantum coherence in double-potential wells in a far-off-resonance magneto-optical lattice.

In addition to these goals, we have pursued new ideas as they emerged, in particular quantum state reconstruction, and the use of atoms in optical lattices to implement qubits, quantum logic and scalable quantum information processing.

### *Summary of Most Important Results*

#### Atom Trapping in Far-Off-Resonance Lattices

We have performed an extensive in-depth study of laser cooling in near-resonance optical lattices, with particular emphasis on the use of magnetic fields to enhance the cooling process and the fraction of atoms prepared in the ground state of the lattice potential (publications [9,11]). We have further developed a method whereby atoms can be adiabatically transferred from a near-resonance optical lattice to a superimposed far-of-resonance lattice with minimal loss and no significant increase in vibrational excitation (publication [10]). These methods are now part of our standard “toolbox” when working with optical lattices.

#### Resolved-Sideband Raman Cooling

A key objective of this proposal has been to develop and experimentally demonstrate a novel method of resolved-sideband Raman cooling, whereby atoms trapped in a far-off-resonance optical lattice can be prepared in a pure quantum state corresponding to the vibrational ground state of the optical potential associated with a single magnetic sublevel. Publication [8] outlines the basic theory, including how one can design optical lattices to achieve appropriate Raman coupling between magnetic sublevels, and how one can use a weak magnetic field to tune this coupling to the first red vibrational sideband as required for cooling. In publication [7], we reported on the first experimental demonstration of this scheme in a two-dimensional lattice,

cooling of order  $10^6$  Cs atoms to the vibrational ground state of the  $6S_{1/2}(F=4, m_F=4)$  hyperfine ground state. A careful measurement showed mean vibrational excitations of  $0.008\pm0.016$  per degree of freedom, corresponding to a population of  $98.4\%\pm3.4\%$  in the two-dimensional vibrational ground state. It is noteworthy that this result was achieved with a very simple experimental setup, which, in contrast to other Raman cooling schemes, did not include separate, phase locked Raman lasers separated by frequencies in the GHz regime.

### Quantum Transport in Mesoscopic Magneto-Optical Double-Well Potentials

Quantum coherence and tunneling of a particle in a double-well potential is central to our understanding of many physical phenomena. We have developed a unique realization of this “toy” model, based on laser cooled Cs atoms in a one-dimensional optical lattice formed by two counterpropagating laser beams with linear polarizations forming an angle  $\theta$ . With the addition of a weak transverse magnetic field, the lowest adiabatic lattice potential forms a periodic array of double-potential wells. The eigenstates of this lattice correspond to spinor wavepackets with highly entangled internal and motional degrees of freedom, allowing us to use the spin as a “meter” to probe the center-of-mass motion (see publication [8]). In publication [1], we describe an experiment in which atoms were initially prepared on one side of the double-well, and subsequently observed to Rabi flop between the two localized states of the ground doublet. Direct examination of the magnetic populations during this oscillation were consistent with a “Schrödinger Cat” -like superposition at the appropriate times. A particularly intriguing aspect of this system is that the dynamics of the corresponding classical system is chaotic (see publication [2]). We are currently improving the experiment with the ultimate goal to study quantum-classical correspondence and quantum feedback control in open quantum systems with nonlinear classical counterparts.

### Reconstruction of the Density Matrix for a Large Angular Momentum

The ability to measure an unknown state of a quantum system forms a necessary complement to quantum state preparation and control. Reconstruction of a (generally mixed) state from repeated measurements of physical observables is, however, a nontrivial task that does not always permit a solution. We have now for the first time demonstrated a general method whereby one can experimentally reconstruct the complete density matrix for a large angular momentum (see publications [2,12,13]). Our reconstruction scheme is based on  $4F+1$  repeated Stern-Gerlach measurements with respect to many different quantization axes. A linear system of equations relates the  $(2F+1)(4F+1)$  measured populations to the  $(2F+1)^2$  elements of the density matrix, and can be solved to find the physical density matrix that best fits the measurements. We have implemented this protocol for laser cooled Cesium atoms in the  $6S_{1/2}(F=4)$  hyperfine ground manifold, and typically reproduce input test states with a fidelity better than 0.95. Our work was motivated in part by the study of quantum transport in magneto-optical lattices, and in part as a tool with which to evaluate the performance and error modes of quantum logic gates for neutral atoms.

## Quantum Information Processing in Optical Lattices

Our original proposal was focused on single-atom manipulation and quantum transport phenomena. In collaboration with Profs. I. H. Deutsch and C. M. Caves at the University of New Mexico, we have discovered that the dipole-dipole interaction between strongly localized wavepackets in principle allows for coherent control of pairs and perhaps larger sets of atoms. We show that this is possible based on a simple scaling argument that compares the dipole-dipole interaction strength with the rate of induced decoherence due to spontaneous emission. In publications [3,4,6] we discuss the prospects for small scale quantum information processing. Neutral atoms in the electronic ground state couple weakly to the environment and allow for long coherence times, and quantum control techniques for trapped neutral atoms may soon rival those demonstrated in ion traps. At the same time, the ability of an optical lattice to trap many atoms while coupling them only as needed should help suppress decoherence and the spread of errors among qubits. With this in mind, we have developed an explicit proposal to use atomic spinor wavepackets as qubits, with the quantum information encoded in pairs of hyperfine ground states. Two independent species of qubits can be trapped in a pair of superimposed lattices with circular polarization of opposite handedness, and moved together in pairs to perform entangling qubit operations. In publication [4], we presented a more complete analysis of the dipole-dipole interaction and its use in several possible entangling protocols. Much theoretical and experimental work remains before one can determine the ultimate merit of these ideas, but so far this entry into the active field of quantum information has sparked considerable interest.

### ***List of Publications and Technical Reports***

- [1] *"Mesoscopic quantum coherence in an optical lattice"*, D. L. Haycock, P. Alsing, I. H. Deutsch, J. Grondalski and P. S. Jessen, Phys. Rev. Lett. **85**, 3365 (2000).
- [2] *"Quantum Transport in Magneto-Optical Double-Potential Wells"*, I. H. Deutsch, P. M. Alsing, J. Grondalski, S. Ghose, P. S. Jessen and D. L. Haycock, J. Opt. B: Quantum Semiclass. Opt. **2**, 633 (2000).
- [3] *"Quantum Computing with Neutral Atoms in an Optical Lattice"*, I. H. Deutsch, G. K. Brennen and P. S. Jessen, Fortschritte der Physik **48**, 925 (2000).
- [4] *"Entangling Dipole-Dipole Interactions and Quantum Logic in Optical Lattices"*, G. K. Brennen, I. H. Deutsch and P. S. Jessen, Phys. Rev. A **61**, 062309-1 (2000).
- [5] *"Sideband Cooling, State Control and Quantum Logic in Optical Lattices"*, I. H. Deutsch, G. K. Brennen, J. Grondalski, C. M. Caves, P. S. Jessen, S. E. Hamann, D. L. Haycock and G. Klose, in *"Laser Spectroscopy, XIV International Conference"*, eds R. Blatt, J. Eschner, D. Liebfried and F. Schmidt-Kaler (World Scientific 1999).
- [6] *"Quantum Logic Gates in Optical Lattices"*, G. K. Brennen, C. M. Caves, P. S. Jessen and I. H. Deutsch, Phys. Rev. Lett. **82**, 1060 (1999).
- [7] *"Resolved-sideband Raman cooling to the ground state of an optical lattice"*, S. E. Hamann, D. L. Haycock, I. H. Deutsch and P. S. Jessen, Phys. Rev. Lett. **80**, 4149 (1998).

- [8] *"Quantum State Control in Optical Lattices"*, I. H. Deutsch and P. S. Jessen, Phys. Rev. A **57**, 1972 (1998).
- [9] *"Enhanced laser cooling and state preparation in an optical lattice with a magnetic field"*, D. L. Haycock, S. E. Hamann, G. Klose, G. Raithel and P. S. Jessen, Phys. Rev. A **57**, R705 (1998).
- [10] *"Atom Trapping in Deeply Bound States of a Far-Off-Resonance Optical Lattice"*, D. L. Haycock, S. E. Hamann, G. Klose and P. S. Jessen, Phys. Rev. A **55**, R3391 (1997).
- [11] *"Temperature and localization of atoms in three-dimensional optical lattices"*, M. Gatzke, G. Birk, P. S. Jessen, A. Kastberg, S. L. Rolston and W. D. Phillips, Phys. Rev. A **55**, R3987 (1997).

### Conference Proceedings

- [12] *"Density matrix reconstruction of atoms with large angular momentum"*, G. Klose, G. A. Smith and P. S. Jessen, QELS 2000, 2000 OSA Technical Digest Series (2000).
- [13] *"Quantum state control via tunneling in an optical potential"*, D. L. Haycock, K. I. Cheong, P. S. Jessen, and I. H. Deutsch, QELS '99, 1999 OSA Technical Digest Series (1999).
- [14] *"Controlling atom-atom interactions in optical lattices"*, G. K. Brennen, C. M. Caves, I. H. Deutsch and P. S. Jessen, QELS '99, 1999 OSA Technical Digest Series (1999).
- [15] *"Coherent quantum tunneling and macroscopic superposition states in optical lattices"*, I. H. Deutsch and P. S. Jessen, IQEC '98, 1998 OSA Technical Digest Series Vol. 7 (1998).
- [16] *"Resolved-sideband Raman cooling in an optical lattice"*, S. E. Hamann, D. L. Haycock, P. S. Jessen and I. H. Deutsch, IQEC '98, 1998 OSA Technical Digest Series Vol. 7 (1998).
- [17] *"Atom trapping in the Lamb-Dicke regime in a far-off-resonance optical lattice"*, D. L. Haycock, S. E. Hamann, G. Klose and P. S. Jessen, Proc. SPIE **2995**, 163 (1997).
- [18] *"Quantum State Preparation in Optical Lattices"*, I. H. Deutsch and P. S. Jessen, QELS '97 Technical Digest Series Vol. 12 (1997).

### Scientific Personnel

#### Graduate Students partially funded by this grant

S. E. Hamann (Ph.D.)  
 D. L. Haycock (Ph.D.)  
 G. Klose  
 K.-I. Cheong  
 G. Smith.

Professor

Poul Jessen

*Report of Inventions*

None

## COLLECTIVE EFFECTS IN ATOM OPTICS

Pierre Meystre

### *Statement of the Problem Studied*

The 1990's have witnessed spectacular advances in atom optics. Following the first demonstrations of Bose-Einstein condensation in low-density atomic vapors in 1995, a large number of experiments have been carried out, including studies of the condensate static and dynamic properties, the investigation of multicomponent condensates, the generation of supercurrents and vortices, etc. In the context of atom optics, the most relevant developments are related to the analogy between the coherent Schrödinger matter waves now available from condensates and coherent electromagnetic waves, leading in particular to the realization of the first "atom lasers", the launching of dark matter wave solitons, and the demonstration of four-wave mixing both between matter waves and between optical and matter waves. Because of the amazing pace of progress and discovery in this field, the wildest theoretical speculations are rapidly turning into experimental reality, and the move from basic studies to first applications is already becoming apparent.

We had pointed out as early as 1993 that two-body collisions play for Schrödinger waves a role completely analogous to that of a nonlinear crystal with cubic (Kerr) nonlinearity in optics. From this observation, it was immediately clear that many of the effects familiar from optics should also take place in ultracold atomic samples. This is the basis of nonlinear atom optics, a new subfield of AMO physics that we have vigorously investigated and promoted in the last few years. Topics of particular interest include, in addition to four-wave mixing, matter-wave phase conjugation, the possibility of programmable matter-wave holographic storage in condensates, as well as the generation of (bright) matter wave solitons using optical fields to tailor the atomic dispersion relation of the atoms and produce negative effective atomic masses. Nonlinear atom optics became an experimental reality in 1999 with experiments on matter-wave four-wave mixing by Phillips et al., and on matter wave superradiance by Ketterle's group, paving the way.

There was initially some question as to the extent to which our work exploited too heavily the analogy between the optical and matter-wave situations. With hindsight, this fear turned out to be unjustified: matter-wave four-wave mixing, including matter-wave superradiance, phase-sensitive matter-wave amplification, and soliton generation rely directly on the optics analogy, which has rapidly turned out to be much more fruitful than even we would have expected.

### *Summary of the Most Important Results*

The last three years has seen a shift of our research toward what we now call "quantum atom optics." Our earlier work on nonlinear atom optics was largely developed in the framework of mean-field theories in which the ultracold atomic sample is described by a Gross-Pitaevskii nonlinear Schrödinger equation. It is, however, well understood that this approach makes important implicit assumptions about the statistical properties of the field and is somewhat similar to the semiclassical approach in nonlinear optics. While describing many effects very accurately, such a description fails in more subtle situations, where the quantum statistical

properties of the field are tantamount. This is true for Maxwell as well as for Schrödinger fields. Indeed, many atom optical situations could benefit substantially from the use of “nonclassical fields.” For instance, atom interferometry using Fock states or squeezed states would beat the standard quantum limit in the detection of feeble signals. Quantum entangled massive particles also show much promise in quantum information processing applications. One established approach to better treat the statistics of the Schrödinger field is the Hartree-Fock-Bogoliubov technique, but it is valid only for small displacements past the “mean-field” behavior of the system.

Inspired by the techniques of theoretical quantum optics, we have promoted an approach based on the selection of “essential modes” to deal with such situations. It allows for a full quantum mechanical treatment of the quantum statistical properties of the matter-wave field, at the expense of replacing a full spatial description of the system by just a few modes. We used this technique to demonstrate the generation of matter-wave squeezing and multimode entanglement in specific nonlinear atom optical systems whose dynamics is governed by spin-changing collisions. In particular, we have recently proposed a method to “mass produce” entangled massive particles in a simple way, which should be amenable to experimental realization in the near future.

One important additional element in discussing nonclassical matter-wave fields consists in formulating an experimentally relevant way to characterize them. We have developed an operational approach to the coherence theory of bosonic atomic fields, introducing different classes of coherence dependent of specific measurement schemes. We have furthermore extended this approach to the characterization of the cross-coherence properties of Schrödinger and Maxwell fields, an important topic in connection with the nonlinear mixing between optical and matter waves.

To see how this mixing works, we remark that much of nonlinear atom optics relies on the observation that two-body collisions are akin to a Kerr-type nonlinearity in nonlinear optics. This analogy is quite profound: the nonlinear polarization serving as a source for the Maxwell field follows from the elimination of the atomic (or crystal) dynamics, resulting in effective nonlinear equations for the field. Likewise, collisions are described by an effective interatomic potential resulting from the (partial) elimination of the electromagnetic field from the system dynamics. As such, nonlinear optics and nonlinear atom optics can be understood as two limits of the same physics.

In general, of course, the situation is more complicated: Neither the matter waves, nor the electromagnetic field can be eliminated from the dynamics. This leads to intriguing new possibilities, including the optical control of matter-wave fields and the nonlinear mixing of optical and matter waves. This also allows the simultaneous amplification of optical and matter waves on Bose-Einstein condensates, as very recently demonstrated by Ketterle's group.

Our work in this direction started in 1997 with the Ph.D. thesis research of Mike Moore. At the time apparently nobody else was thinking of coherently mixing of optical and Schrödinger matter waves. The seed money provided by JSOP was particularly welcome in initiating such highly speculative research. We initially considered a situation where an optical cavity selected

just one mode of the electromagnetic field. This model, an ultracold atoms version of the Collective Atomic Recoil Laser (CARL), demonstrated some of the promises of the nonlinear mixing between optical and matter waves, including the optical control of the quantum statistical properties of Schrödinger fields, the phase-sensitive amplification of matter waves, and the quantum entanglement between optical and matter waves. Yet, this all seemed rather unrealistic.

However, shortly after completion of this original work the MIT group demonstrated experimentally the coherent four-wave mixing between atoms and light: in fact, an optical cavity is not even needed to select specific optical modes: using a cigar-shaped condensate, they demonstrated the four-wave mixing of optical and matter waves, leading to the generation of a sequence of matter-wave sidemodes. This effect, called matter-wave superradiance, results from the fact that for an appropriate polarization of the laser beam incident on the condensate, spontaneous emission is preferentially along its long axis. This leads to the creation of a matter-wave density grating that survives much longer than the transit time of light through the condensate, and provides a feedback mechanism that enhances the subsequent light scattering. It was a straightforward task to extend our theory of the CARL to describe that situation, including a detailed analysis of the shot-to-shot fluctuations in the dynamics of the system. We have also analyzed how this system can be used to generate a quantum entanglement between optical and matter-wave fields, a feature of considerable potential interest in the emerging field of quantum information processing.

To sum up, then, these have been a very successful and exciting three years. We foresee that future work will develop on several fronts: first, there will be further emphasis toward the generation and characterization of nonclassical matter-wave fields. Second, applications of atom optics in systems such as inertial sensors, gravimeters and gravity gradiometers will take center stage. And finally, fermionic fields will gain in importance. We have recently demonstrated that nonlinear atom optics with fermions is also possible. This opens up a number of fascinating new directions, including “fermionic atom lasers”, the use of Pauli blockade to generate strongly nonclassical fields, the mixing between bosonic and fermionic fields, and much more. We fully intend to maintain a leading role in the investigation of these new directions.

#### ***List of Publications and Technical Reports***

1. M. G. Moore and P. Meystre, “Effects of atomic diffraction on the collective atomic recoil laser”, *Phys. Rev. A* **58**, 3248 (1998).
2. E. V. Goldstein, O. Zobay and P. Meystre, “Coherence of atomic matter-wave fields”, *Phys. Rev. A* **58**, 2373 (1998).
3. E. V. Goldstein, E. M. Wright and P. Meystre, “Detection of condensate vortex states”, *Phys. Rev. A* **58**, 576 (1998).
4. O. Zobay and P. Meystre, “Phase dynamics in a binary-collision atom-laser scheme”, *Phys. Rev. A* **57**, 4710 (1998).

5. E. V. Goldstein and P. Meystre, "Atomic detection and matter-wave coherence", *Phys. Rev. Lett.* **80**, 5036 (1998).
6. E. V. Goldstein, E. M. Wright and P. Meystre, "Dressed Bose-Einstein condensates in high-Q cavities", *Phys. Rev. A* **57**, 1223 (1998).
7. M. Guzman and P. Meystre, "Dynamical effects of the dipole-dipole interaction in 3-dimensional optical lattices", *Phys. Rev. A* **57**, 1139 (1998).
8. E. V. Goldstein and P. Meystre, "Phase conjugation of multicomponent Bose-Einstein condensates", *Phys. Rev. A* **59**, 1509 (1999).
9. O. Zobay, E. M. Wright and P. Meystre, "Creation of gap solitons in Bose-Einstein condensates", *Phys. Rev. A* **59**, 643, (1999).
10. M. G. Moore and P. Meystre, "Optical control and entanglement of atomic Schrödinger fields", *Phys. Rev. A* **59**, R1754 (1999).
11. E. V. Goldstein and P. Meystre, "Quantum theory of atomic four-wave mixing in Bose-Einstein condensates", *Phys. Rev. A* **59**, 3896 (1999).
12. G. J. Yang, O. Zobay and P. Meystre, "Two-atom dark states in electromagnetic cavities", *Phys. Rev. A* **59**, 4012 (1999).
13. M. G. Moore, O. Zobay and P. Meystre, "Quantum optics of a Bose-Einstein condensate coupled to a quantized light field", *Phys. Rev. A* **60**, 1491 (1999).
14. E. S. Lee, C. Geckeler, J. Heurich, A. Gupta, Kit-Iu Cheong, S. Secrest and P. Meystre, "Dark states of dressed Bose-Einstein condensate", *Phys. Rev. A* **60**, 4006 (1999).
15. O. Zobay, E. V. Goldstein and P. Meystre, "Atom holography", *Phys. Rev. A* **60**, 3999 (1999).
16. G. A. Prataviera, E. V. Goldstein and P. Meystre, "Mutual coherence of optical and matter waves", *Phys. Rev. A* **60**, 4846 (1999).
17. M. G. Moore and P. Meystre, "Theory of superradiant scattering of laser light from Bose-Einstein condensates", *Phys. Rev. Lett.* **83**, 5202 (1999).
18. P. Meystre, "Amplifier means gains for atom optics", *Physics World* **13**, 24 (2000).
19. E. V. Goldstein, M. G. Moore and P. Meystre, "Nonlinear manipulation and control of matter waves", *Laser Physics* **10**, 8 (2000).
20. J. Heurich, M. G. Moore and P. Meystre, "Cavity Quantum Optics and the 'Free-Atom Laser', " *Optics Commun.* **179**, 549 (2000).

21. E. V. Goldstein, M. G. Moore and P. Meystre, "Nonlinear optics of matter waves", in *Advances in Laser Physics*, edited by V. S. Letokhov and P. Meystre, Laser Science and Technology Second Series Volume 1, Harwood Academic Publishers, Amsterdam (2000), p. 117.
22. G. Prataviera, J. Zapata and P. Meystre, "Higher-order mutual coherence of optical and matter waves", *Phys. Rev. A* **62**, 023605 (2000).
23. H. Pu and P. Meystre, "Creating macroscopic atomic EPR states from Bose-Einstein condensates", *Phys. Rev. Lett.* **85**, 3987 (2000).
24. S. Pötting, E. S. Lee, W. Schmitt, I. Rumyantsev, B. Mohring and P. Meystre, "Quantum coherence and interaction-free measurements", to be published in *Phys. Rev. A*, Rapid Commun.
25. J. Heurich, H. Pu, M. G. Moore and P. Meystre, "Instabilities and self-oscillations in atomic four-wave mixing," to be published in *Phys. Rev. A*.
26. E. V. Goldstein, M. G. Moore, H. Pu and P. Meystre, "Eliminating the mean-field shift in Bose-Einstein condensates," to be published in *Phys. Rev. Lett.*
27. S. Pötting, O. Zobay, P. Meystre and E. M. Wright, "Magneto-optical control of bright atomic solitons", to be published in *J. Mod. Optics*.
28. M. G. Moore and P. Meystre, "Generating atom-photon pairs from Bose-Einstein condensates," to be published in *Phys. Rev. Lett.*

### **Books**

- "Elements of Quantum Optics", 3rd Edition, Springer Verlag, Berlin (1998). This third edition includes new chapters on atom optics and cavity quantum electrodynamics, as well as expanded discussions of quantum mechanics, system-reservoir interactions and second quantization.
- V. S. Letokhov and P. Meystre, editors, "Advances in Laser Physics," Harwood Academic Publishers, Amsterdam (2000).

### **Invited Presentations**

1. P. Meystre, "Ultracold regime of the collective atom recoil laser", CAS Workshop on Quantum Control of Atomic Motion, Albuquerque, NM (1998).
2. P. Meystre, "Coherence of matter waves", ONR and TAMU Workshop on Quantum Optics, Jackson Hole, WY (1998).

3. M. G. Moore and P. Meystre, "The collective atomic recoil laser: Dynamically coupled coherent Maxwell and Schrödinger fields", ONR and TAMU Workshop on Quantum Optics, Jackson Hole, WY (1998).
4. P. Meystre, "Coherence theory of matter waves", Third Ibero-American Optics Meeting and 6th Latin-American Meeting on Optics, Lasers, and Their Applications, Cartagena de Indias, Colombia, (1998).
5. P. Meystre, "Two-atom dark states in optical resonators", 29<sup>th</sup> Winter Colloquium on Quantum Electronics, Snowbird, UT (1999).
6. P. Meystre, "Matter-wave phase conjugation", 29<sup>th</sup> Winter Colloquium on Quantum Electronics, Snowbird, UT (1999).
7. P. Meystre, "From optics to atom optics: A case study of the interplay between theory and experiment and its technological applications", ITAMP Workshop on "The Role of Theory in AMO Physics", Cambridge, MA (1999).
8. E. V. Goldstein and P. Meystre, "Recent progress in nonlinear atom optics", 8th International Laser Physics Workshop LPHYS '99, Budapest, Hungary (1999).
9. P. Meystre, "From free-electron lasers to matter-wave 'superradiance' --- 25 Years of physics with Marlan Scully", Modern Trends in Quantum Optics, Garching, Germany (1999).
10. M. G. Moore and P. Meystre, "Optical control and entanglement of matter-wave fields", 8th International Laser Physics Workshop LPHYS '99, Budapest, Hungary (1999).
11. P. Meystre, "Nonlinear manipulation and control of matter waves", TAMU-ONR Workshop on Quantum Optics, Jackson Hole, WY (1999).
12. P. Meystre, "Nonlinear atom optics", International Conference on Laser Physics and Quantum Optics, Shanghai, China (1999).
13. P. Meystre, "Elimination of the collisional mean-field shift in multicomponent Bose-Einstein condensates," RTC/ITAMP Workshop on "Multicomponent and Spinor Bose-Einstein Condensates of Trapped Dilute Vapors," Rochester (NY) 2000.
14. M. G. Moore and P. Meystre, "Elimination of the mean-field shift in multicomponent Bose-Einstein condensates," Snowbird (UT) 2000.
15. P. Meystre, "Dressed Bose-Einstein condensates," ITAMP Workshop on "Physics and Applications of 'Slow' Light," Cambridge (MA) 2000.
16. P. Meystre, "Atom optics", Lectures series, 2000 Quantum Optics Theory Workshop, University of Texas at Austin, Austin (TX) 2000.

17. P. Meystre, "Superradiant scattering from Bose-Einstein condensates", American Physical Society, DAMOP Annual Meeting, Storrs (CT) 2000.
18. P. Meystre, "Quantum coherence in quantum and atom optics", QUEST 2000 Workshop, Santa Fe (NM) 2000.
19. P. Meystre, "Recent advances in nonlinear atom optics", TAMU/ONR Workshop on Quantum Optics, Jackson Hole Resort (WY) 2000.
20. M. G. Moore and P. Meystre, "Atomic four-wave mixing: fermions vs. bosons", TAMU/ONR Workshop on Quantum Optics, Jackson Hole Resort (WY) 2000.
21. S. Pötting and P. Meystre, "Quantum coherence and interaction-free measurements", TAMU/ONR Workshop on Quantum Optics, Jackson Hole Resort (WY) 2000.
22. P. Meystre, "Nonlinear wave mixing and matter-wave amplification", Quantum Optics I, Santiago, Chile, 2000.
23. P. Meystre, "Marginally acceptable personal, anecdotal and technical remarks on Joe Eberly, Cavity QED, and Atom Optics", Quantum Control of Atoms and Fields, a Symposium in Honor of J. H. Eberly, Rochester (NY), 2000.

#### ***Contributed Presentations***

1. E. V. Goldstein, E. M. Wright and P. Meystre, "Atomic detection and matter-wave coherence", DAMOP 98, Santa Fe, NM (1998).
2. M. G. Moore and P. Meystre, "Matter wave optics theory of the collective atomic recoil laser", DAMOP 98, Santa Fe, NM, (1998).
3. O. Zobay and P. Meystre, "First-order correlation functions in a binary-collisions atom laser scheme", DAMOP 98, Santa Fe, NM, (1998).
4. E. V. Goldstein, O. Zobay and P. Meystre, "Coherence of matter waves", Workshop on Quantum Gases, Konstanz, Germany, (1998).
5. M. G. Moore and P. Meystre, "The BEC/CARL Laser: Dynamically coupled Schrödinger and Maxwell fields", Workshop on Quantum Gases, Konstanz, Germany (1998).
6. O. Zobay, S. Pötting, E. M. Wright and P. Meystre, "Gap solitons in Bose-Einstein condensates", DAMOP '99, Atlanta (1999).
7. M. G. Moore and P. Meystre, "Quantum entanglement and control of coherence between a condensate and an optical field", DAMOP '99, Atlanta (1999).

8. G. Yang, O. Zobay and P. Meystre, "Two-atom dark states in electromagnetic cavities", DAMOP '99, Atlanta, (1999).
9. J. Heurich, M. G. Moore and P. Meystre, "Matter-wave cavity effects in the optical control of condensates", DAMOP '99, Atlanta (1999).
10. E. V. Goldstein and P. Meystre, "Quantum theory of atomic four-wave mixing in Bose-Einstein condensates", DAMOP '99, Atlanta (1999).

***Scientific Personnel***

**Graduate Students partially supported by this grant**

Paul Pax, Ph.D. 1998

Michael Moore, Ph.D. 2000

Jan Heurich

Scott Secrest

**Research Intern**

Jesus Zapata

**Research Associates**

Elena V. Goldstein

Oliver Zobay

**Professor**

Pierre Meystre

***Report of Inventions***

"Quantum Microfabrication by Matter-wave or Optical Holography", P. Meystre, M. Moore, O. Zobay, November 16, 1998.

# DESIGN OPTIMIZATION OF CIRCULAR GRATING DBR LASERS FOR HIGH POWER APPLICATIONS

Mahmoud Fallahi

## *Statement of the Problem Studied*

In this report, we report the design, fabrication, and characterization of circular-grating surface-emitting lasers (CG-SELs) for use in free space optical communications. We report low divergence, high power output, and show dynamic control over beam characteristics, including beam steering and wavelength tuning. Several material structures and cavity designs were explored to maximize lasing characteristics for a particular application. We have achieved the highest power for CG-SELs to date (220 mW at 600 mA) and external quantum efficiencies of 34%. Additionally, beam steering was achieved using a novel method of changing carrier and temperature characteristics within the gratings, using a transparent electrode (in this case ITO). Shifts in excess of 1° were attained. Using a similar technique, 1 nm wavelength tuning was achieved.

Due to simple geometrical considerations, it is difficult for typical edge-emitting semiconductor lasers to meet the requirements for integration into some optical systems. Because edge-emitting lasers require a cleaved edge for operation and power extraction, 1D arrays, known as “laser bars”, are feasible. However, higher dimensions are impossible to achieve without complex mounting considerations. Additionally, edge-emitting lasers suffer from beam ellipticity because of the high confinement in the epitaxial growth direction. Vertical-Cavity Surface-Emitting Lasers (VC-SELs) are able to meet both of these requirements, but the small interaction with the active area prevents VC-SELs from achieving high power. Additionally, VC-SELs are difficult to increase in the transverse extent due to inhomogeneous pumping profiles. Both edge-emitting lasers and VC-SELs are also impossible to steer without moving parts. Furthermore, wavelength tuning in edge emitting lasers, as well as VC-SELs, is usually considered as a problem, because the majority of wavelength tuning is due to temperature changes within the cavity itself, and only changes with driving current.

CG-SELs on the other hand, circumvent some of these problems by using grating-coupling to take a horizontal mode (guided in the epitaxial structure), and extract it from the surface of the semiconductor. Because the output is large, there is low beam divergence. Additionally, the horizontal cavity allows for large mode interaction with the gain medium. These cavity designs make it possible to reach high power, at least an order of magnitude higher than VC-SELs. CG-SELs can fulfill requirements for free-space optical interconnects, opto-electronic integration, optical data storage, and optical switching.

## *Summary of the Most Important Results*

### *Epitaxial Structure*

For this project, a triple quantum well structure was designed and used (figure 1). Incorporated in this structure is an etch-stop layer that is situated appropriately on the p-side to position the

gratings very accurately relative to the active layer structure. This etch-stop is essential for accurate positioning and device reproducibility, as well as efficient coupling of the mode. One problem with grating coupling is that there is typically an additional substrate mode emitted that is traditionally difficult to use, and results in power loss. To avoid this, a  $\lambda/4$  stack is included on the n-side to reflect the substrate mode, creating useful extraction of this substrate mode.

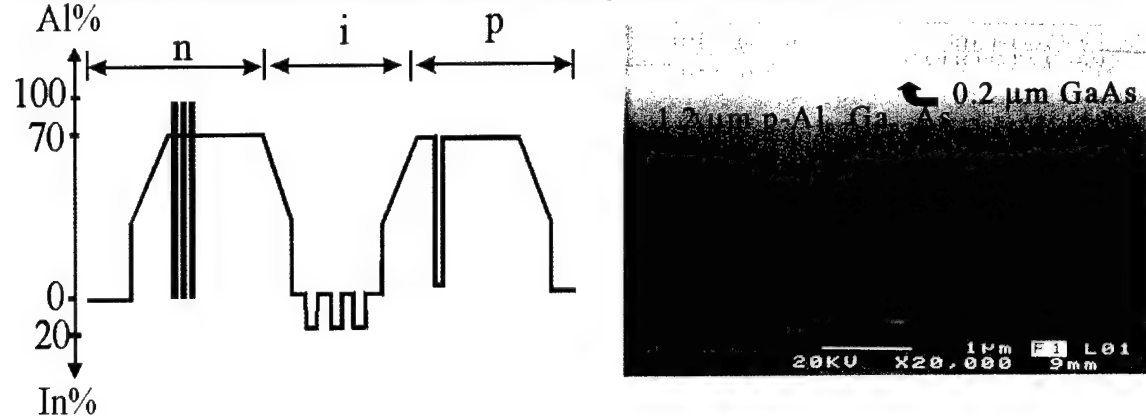


**Figure 1. Layer structure designed for CG-SELs, and micrograph of same**

### Fabrication

The grating section, which is passive in DBR devices, is designed to reduce non-radiative recombination. The grating period that sets the lasing wavelength is red-shifted with respect to the gain peak. This results in a reduction of the material absorption, making the grating section essentially transparent. It is possible to use pure second-order gratings ( $\sim 300$  nm period), which provide both feedback and surface-normal emission in the same section. A combination of first ( $\sim 150$  nm period) and detuned-second-order gratings ( $\sim 280$  nm period), which provide feedback, and non-normal emission, respectively (figure 2) is also used for further functionality.

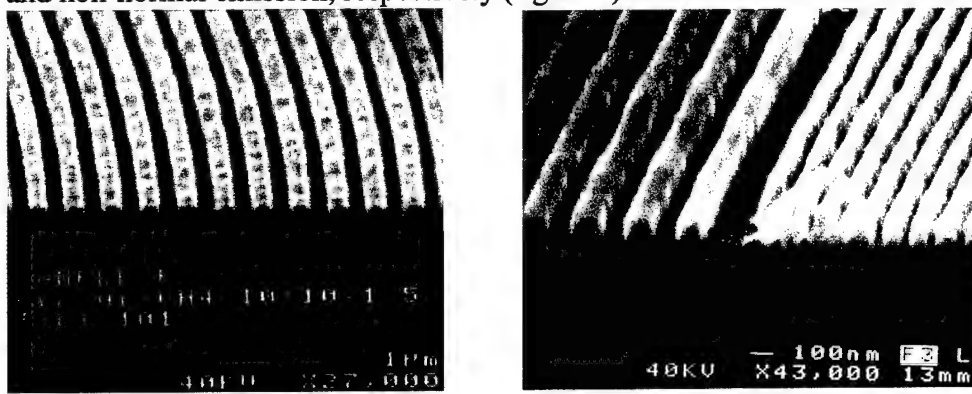


**Figure 2. DBR, pure second order (left) and first and detuned second order (right) grating**

Pure second order grating is necessary for wavelength tuning *without* beam steering. First and detuned second order gratings are necessary for beam steering, as well as facilitating non-normal emission such as focusing.

For functionality, a 200 nm film of ITO is deposited on the sample, patterned and etched away, resulting in ITO remaining on the desired gratings used to facilitate either wavelength tuning

(ITO on pure second-order gratings) or beam steering (ITO on detuned second-order gratings with bare first order gratings).

### *Power and Beam Characteristics*

With a combination of an optimized layer structure, grating positioning, fabrication refinements, and grating design improvements, considerable improvements were obtained compared to previous CG-SEL results. L-I curves indicate a peak power of 225 mW at a drive current of 600 mA (figure 3).

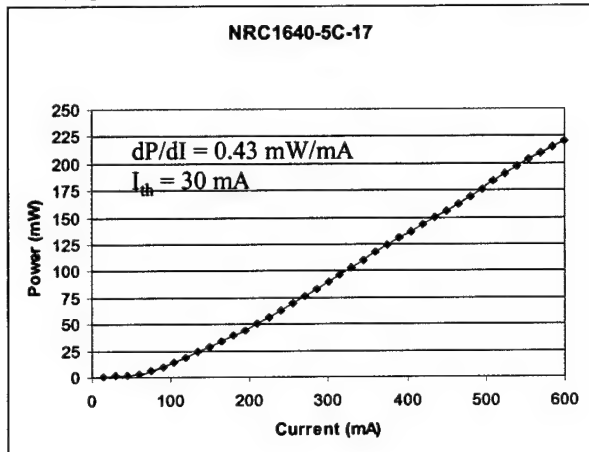


**Figure 3. LI Curve for high power CG-SEL**

The far-field characteristics (figure 4) show that for high-power operation, there is quasi-uniform emission, resulting in a quasi-circular far field with a 1° divergence angle.

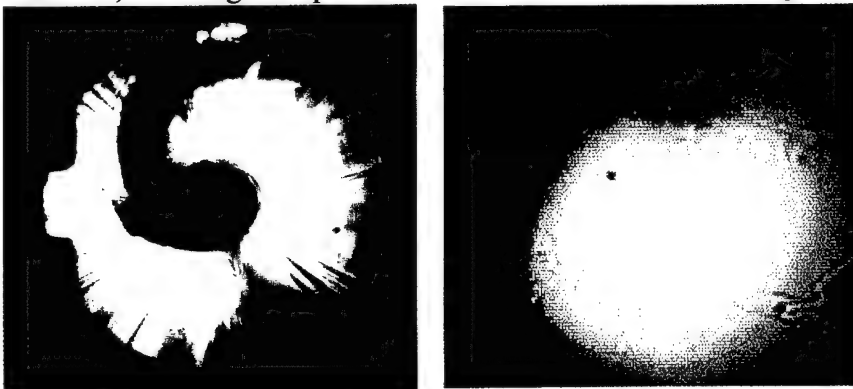


**Figure 4. Near (left) and Far (right) field of CG-SEL**

Spectral characteristics indicate that this is operating in multiple modes centered around 983 nm, and approximately 1 nm wide maximum. Devices designed for beam steering were designed to operate with near-single mode operation, specifically in  $m=1$  Hankel mode that corresponds to the only CGSEL azimuthal mode without an on-axis null in the far field.

### *Functionality (Wavelength Tuning and Beam Steering)*

Wavelength tuning is achieved through ITO current injection into the passive grating section. 1 nm wavelength tuning is achieved (figure 5). There is a longitudinal mode hop in the middle, but no steering or far field change is observed.

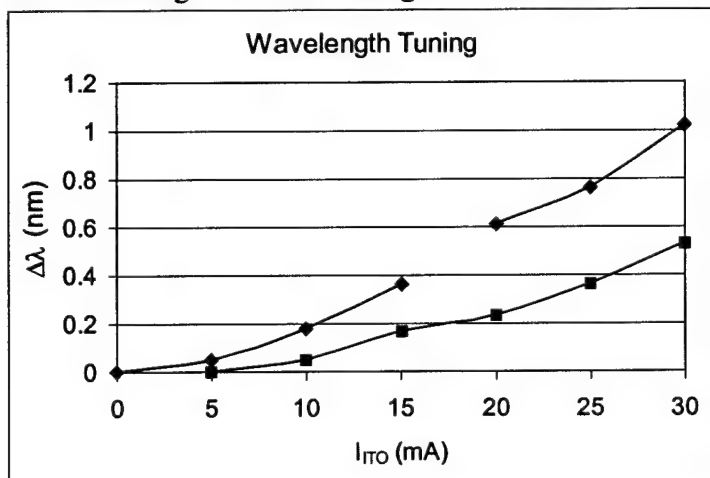


**Figure 5. Wavelength shift (blue is forward bias, red is reverse bias) of CG-SEL**

This wavelength tuning is attributed primarily to thermal effects, although there is a non-zero tuning due to increased carrier populations. Future work will hopefully reduce the temperature effects so that the carrier effects will dominate, resulting in significantly faster modulation.

Beam steering occurs when ITO is patterned only on detuned second-order gratings. Theory indicates, and experiment confirms that a blue shift detuning from the lasing wavelength allows a higher  $d\theta/dI$ . In this experiment, we achieved more than  $1^\circ$  steering.

### *List of Publications and Technical Reports*

1. S. Penner, R. Bedford, H. Luo, S. Mendes and M. Fallahi, "High Power Wavelength Tunable Circular Grating Surface Emitting DBR Lasers" *Applied Physics Lett.* Vol.76, March 2000, pp. 1359-1361.
2. M. Fallahi, "Grating Coupled Surface Emitting Quantum Well Semiconductor Lasers," invited paper, CLEO/Pacific, September 2, 1999. Seoul, Korea.
3. S. Penner, M. Fallahi, O. Nordman "Electron, cyclotron resonance reactive ion etching of GaAs in  $\text{Cl}_2:\text{CH}_4$  mixture," *Microelectronic Engineering* vol. 41/42, April 1998, pp. 383-386.
4. M. Fallahi, K. Kasunic, S. Penner, O. Nordman and N. Peyghambarian, "Design and fabrication of circular grating coupled distributed Bragg reflector lasers," *Optical Engineering* vol. 37, April 1998, pp. 1169-1174.

5. K. Kasunic, M. Fallahi, "Gain Saturation in circular-grating distributed-feedback semiconductor lasers," J. Opt. Soc. Am.-B vol. 14, 1997, p. 2147.

***Scientific Personnel***

**Graduate Students partially supported by this grant**

Scott Penner (Ph.D. 1999)

Hui Luo (Ph.D. 2000)

Ravil Latipov (M.S. 1998)

Robert Bedford

**Professor**

Mahmoud Fallahi

***Report of Inventions***

"Electrically Steerable High Power Surface Emitting Lasers," M. Fallahi, Provisional Patent, UA# 1817 (1999).

# COHERENT AND INCOHERENT ULTRAFAST NONLINEAR OPTICAL PROCESSES IN ANISOTROPICALLY STRAINED SEMICONDUCTOR QUANTUM WELLS

Rudolf H. Binder

## *Statement of the Problem Studied*

This project contained two closely related theoretical investigations in the area of semiconductor optics. First, linear and nonlinear optical properties of semiconductor quantum wells were studied on the basis of a microscopic many-body theory, and, secondly, a theoretical approach to vertical-cavity surface-emitting lasers (VCSELs) with special emphasis on vectorial lasing modes has been developed.

A major goal of this project was to provide a microscopic theory of certain opto-electronic devices that contain uniaxially strained semiconductor quantum wells. A specific example for such a device is a VCSEL in which the active material (a semiconductor quantum well) exhibits accidental (i.e., unintentional) uniaxial strain. The motivation underlying this goal was the realization that phenomenological theories of such devices can only be applied if suitable fits (using fitting parameters) to the specific device have been made. In other words, phenomenological theories are not applicable to a large class of devices and are not strictly predictive. In contrast, microscopic theories are generally predictive and contain only material parameters for the given semiconductor material. With such input, they can be applied to a large class of opto-electronic devices covering, in our case, both VCSELs and normal-incidence light modulators.

To approach this goal, a number of issues had to be addressed.

A microscopic theory for the linear and nonlinear optical response of semiconductor quantum wells had to be developed. While the ultimate goal was the description of uniaxially strained quantum wells, the theoretical investigation had to include the physics of non-strained quantum wells as well, because non-strained quantum wells offer a much wider array of theory-experiment comparisons which is important for a correct assessment of the applicability of the theory. This is true in particular for ultrafast optical nonlinearities, which constitute the main test bed of the developed many-body theory. In addition to general many-body effects underlying the optical nonlinearities, the inclusion of strain effects was an important aspect of this project. Technically, strain effects are related to the bandstructure of the crystal, which makes it necessary to unify the anisotropic bandstructure with many-body effects such as excitonic effects or electron-hole plasma effects.

In order to provide a unified microscopic theory of VCSELs with uniaxially strained semiconductor quantum wells, the issue of vectorial electromagnetic eigenmodes in semiconductor microcavities had to be addressed. This part of the project dealt with the light propagation in both; empty cavities (which defined the so-called cold-cavity modes) as well as cavities subject to the nonlinear feedback of the active material (the semiconductor quantum well). A major issue within our project was the derivation and complete classification of

vectorial cold-cavity modes, as well as the verification and test of our theory through suitable theory-experiment comparisons.

Finally, to obtain a complete theory for electrically pumped VCSELs, the extension of the microscopic quantum well theory to the case of electrically pumped laser operation had to be made. This final theory was designed to yield predictions for vectorial mode stability in VCSELs with nothing more than standard material parameters, such as bandstructure (Luttinger) parameters and elements of the elastic compliances tensor, as input parameters.

### ***Summary of the Most Important Results***

As stated in the previous section, the project contained theoretical investigations in a number of areas, ranging from fundamental many-body effects in non-strained semiconductor quantum wells to predictive device-modeling theories.

Basic issues in the many-body theory of semiconductor quantum wells have been addressed in Refs. [2,4,9,12-16,18-22]. Within the context of this project, these studies provide insight into the basic excitonic and electron-hole plasma effects on a Hartree-Fock or statically-screened Hartree-Fock level. Since the effects of uniaxial strain require a good understanding of heavy-hole-light-hole band coupling effects, the studies published in Refs. [12,13,16,22], which are all done for case without uniaxial strain, provide the general theory and understanding of optical nonlinearities based on heavy-hole-light-hole band coupling effects. In these publications, we have shown how to incorporate these band coupling effects into a theory for excitonic nonlinear optical response. In other words, we have unified excitonic Coulomb interaction effects and the heavy-hole-light-hole Luttinger Hamiltonian and we have also learned and shown how to approach this problem numerically. An important feedback for our theoretical approach, which is based on suitable extensions of the semiconductor Bloch equations, through experiment-theory comparison was provided by the possibility to investigate excitonic Rabi oscillations [14-16,18-21]. This experiment-theory comparison shows clearly the principle validity of our microscopic many-body theory.

The central foundation of this project is the theory we developed for the optical nonlinear response of uniaxially strained quantum wells. This theory combines the uniaxially strain effects entering the Luttinger Hamiltonian for the valence band structure with the excitonic and electron-hole plasma many-body effects evaluated here on a statically-screened Hartree-Fock level. The numerical evaluation of this theory led to the prediction of a new nonlinear optical effect, namely that of interaction-induced polarization rotation [3]. Here, the excitonic local field effects modify the generalized polarization rotation (more precisely: the polarization trajectories in the Poincare plane) and hence determine the polarization characteristics of the transmitted or reflected light pulse depending, in a non-trivial way, on the input light polarization and intensity parameters. The Hartree-Fock theory was also modified and extended to incorporate biexcitonic correlation effects, which turned out to be important for the understanding of the ultrafast anisotropic optical Stark effect [8], which had been observed in experimental investigations in the Army Research Laboratories in the group of Dr. Michael Wraback.

The second, device-oriented aspect of this project was in the area of VCSEL modeling. Here, we have developed a general anisotropic vectorial VCSEL model.

To this end, we had to solve Maxwell's equations in a semiconductor microcavity and to derive, define and categorize the vectorial eigenmodes of the systems. We did this on the basis of a generalized transfer matrix approach, which combines the solutions for fiber-optical hybrid modes with the specific DBR (distributed-Bragg reflector) structure of the microcavity mirrors [1,5,10,11]. Our theory for these general vectorial eigenmodes has been tested and verified in a theory-experiment comparison using commercially available VCSELs produced by Motorola Inc. [6,7]. This JSOP-investigation obtained additional funding through a one-time grant by Motorola Inc., Phoenix Applied Research Center.

Finally, we have investigated vectorial stability criteria of VCSELs with anisotropically strained quantum wells as active material [17,23-25]. These investigations include a microscopic theory for the active material such as bandstructure effects, Coulomb-interaction effects, anisotropic optical matrix elements, anisotropic phase-space blocking and spectral hole burning, as well as electrical-pumping within the Chow-Koch-Sargent model, and the vectorial VCSEL modes discussed above. Our theory can be viewed as a comprehensive microscopic model for vectorial mode properties of VCSELs in cw (continuous wave) operation. It provides the microscopic generalization and justification for the widely-used SFM (San Miguel-Feng-Moloney) model, and it shows how the vectorial stability can be predicted with nothing more than material parameters such as elastic compliances as theoretical input. In specific limiting cases, the results agree qualitatively with the SFM model, but they also provide a way to understand the polarization stability on the basis of the material properties underlying the anisotropic optical nonlinear response.

#### *List of Publications and Technical Reports*

1. D. Burak and R. Binder, "Cold-cavity vectorial eigenmodes of VCSELs", *IEEE J. Quant. Elect.* **33**, 1205-1214 (1997).
2. R. Binder, H.S. Köhler, M. Bonitz, and N. Kwong, "Green's function description of momentum orientation relaxation of photo-excited electron plasmas in semiconductors", *Phys. Rev. B* **55**, 5110-5116 (1997).
3. R. Binder, "Interaction-induced polarization rotation in anisotropic semiconductor quantum wells", *Phys. Rev. Lett.* **78**, 4466-4469 (1997).
4. H.S. Köhler and R. Binder, "The interplay of electron-phonon and electron-electron scattering within the two-time Green's function description", *Contrib. Plasma Phys.* **37**, 167-172 (1997).
5. D. Burak and R. Binder, "Electromagnetic characterization of vertical-cavity surface-emitting lasers based on a vectorial eigenmode calculation", *Appl. Phys. Lett.* **72**, 891-893 (1998).

6. D. Burak, S.A. Kemme, R.K. Kostuk, and R. Binder, "Identification of lasing modes of index-guided VCSELs under DC injection conditions", *Appl. Phys. Lett.* **73**, 3501-3503 (1998).
7. T. Milster, W. Jiang, E. Walker, D. Burak, P. Claisse, P. Kelly, and R. Binder, "A single-mode high-power vertical-cavity surface-emitting laser", *Appl. Phys. Lett.* **72**, 3425-3427 (1998).
8. M. Wraback, H. Shen, J. Pamulapati, P.G. Newman, R. Binder, and M. Dutta, "Femtosecond studies of the excitonic optical Stark effect in an anisotropically strained multiple quantum well", 194th meeting of The Electrochemical Society, Boston, Massachusetts, November 1-6, 1998, paper 991.
9. R. Binder and M. Lindberg, "Ultrafast adiabatic population transfer in p-doped semiconductor quantum wells", *Phys. Rev. Lett.* **81**, 1477-1480 (1998).
10. D. Burak and R. Binder, "Theoretical Analysis of polarization properties of VCSEL eigenmodes", contributed talk, *Physics and Simulation of Optoelectronic Devices VI, OE '98*, San Jose, California, 24-30 January 1998 (SPIE Proceedings Vol. 3283).
11. D. Burak and R. Binder, "Full vectorial eigenmode analysis of VCSELs: threshold gain values and modal frequencies", contributed talk, *Vertical Cavity Surface Emitting Lasers II, OE '98*, San Jose, California, 24-30 January 1998 (SPIE Proceedings Vol. 3286).
12. R. Binder and M. Lindberg, "Ultrafast adiabatic population transfer in p-doped semiconductor quantum wells", contributed talk, in: *Bulletin of the American Physical Society*, Vol. 43, No. 1, 765 (1998).
13. R. Binder and M. Lindberg, "Ultrafast adiabatic population transfer in p-doped semiconductor quantum wells", contributed talk, paper QWE8, *International Quantum Electronic Conference IQEC 1998*, San Francisco, CA, May 3-8, 1998.
14. A. Schülzgen, R. Binder, M. Donovan, M. Lindberg, K. Wundke, H. Gibbs, G. Kithrova, N. Peyghambarian, "Direct observation of light-induced Rabi oscillations in semiconductors", *Phys. Rev. Lett.* **82**, 2346-2349 (1999).
15. Schülzgen, R. Binder, M. Donovan, K. Wundke, H. Gibbs, G. Kithrova, N. Peyghambarian, and M. Lindberg, "Excitonic Rabi oscillations in semiconductors", *Optics and Photonics News*, Vol. 10, No. 12, 39-40 (1999).
16. R. Binder, "Rabi oscillations and Raman coherences in semiconductor quantum wells", paper QMC4, *Quantum Electronics and Laser Science Conference (QELS '99)*, Baltimore, Maryland, May 25-27, 1999.

17. D. Burak, J. Moloney, and R. Binder, "Microscopic model for polarization switching in optically anisotropic VCSELs", Vertical Cavity Surface Emitting Lasers III, OE '99, San Jose, California, 25-26 January 1999 (SPIE Proceedings Vol. 3627).
18. R. Binder, "Rabi Oscillations in Semiconductors", 29th Winter Colloquium on the Physics of Quantum Electronics (PQE), Snowbird, Utah, January 3-6, 1999.
19. M. Donovan, A. Schülzgen, K. Wundke, R. Binder, M. Lindberg, H. M. Gibbs, G. Kithrova, and N. Peyghambarian, "Experimental observation of multiple excitonic Rabi oscillations in a semiconductors", Ultrafast Phenomena in Semiconductors III, OE '99, San Jose, California, 27-29 January 1999 (SPIE Proceedings Vol. 3624).
20. R. Binder, M. Lindberg, A. Schülzgen, M. Donovan, K. Wundke, H. M. Gibbs, G. Kithrova, and N. Peyghambarian, "Many-body aspects of excitonic Rabi oscillations in semiconductors", Physics and Simulation of Optoelectronic Devices VII, OE '99, San Jose, California, 25-29 January 1999 (SPIE Proceedings Vol. 3625).
21. Schülzgen, R. Binder, M. Donovan, M. Lindberg, K. Wundke, and N. Peyghambarian, "Laser-induced Rabi oscillations in semiconductors", paper QMC5, Quantum Electronics and Laser Science Conference (QELS '99), Baltimore, Maryland, May 25-27, 1999.
22. R. Binder and M. Lindberg, "Three-band excitonic Rabi oscillations in semiconductor quantum wells", Phys. Rev. B **61**, 2830-2836 (2000).
23. D. Burak, J.V. Moloney and R. Binder, "Microscopic theory of polarization properties of optically anisotropic vertical-cavity surface-emitting lasers", Phys. Rev. A **61**, 53809-53830 (2000).
24. D. Burak, J.V. Moloney and R. Binder, "Macroscopic vs. microscopic description of polarization properties of optically anisotropic vertical-cavity surface--emitting lasers", IEEE J. Quant. Elect. **36**, 956-970 (2000).
25. D. Burak, and R. Binder, "A microscopical model for polarization stability in optically anisotropic VCSELs", Conference on Physic and Simulation of Optoelectronic Devices, Photonics West 2000, San Jose, California, 22-28 January 2000 (SPIE Proceedings Vol. 3944).

### ***Scientific Personnel***

#### **Graduate students partially funded by this grant**

Ilya Rumyantsev  
Zhenshan Yang

Research Associate

Dariusz Burak

Professor

Rudolf Binder

***Report of Inventions***

None

## **PORABLE MWIR COMPUTED TOMOGRAPHY IMAGING SPECTROMETER (CTIS)**

Michael Descour

### ***Statement of the Problem Studied***

An imaging spectrometer measures both the spatial and spectral content of an object scene. In contrast with classical, broadband imaging, the spectral information permits the classification of portions of the scene based upon material content or temperature. The cubic ( $x, y, \lambda$ ) object for an imaging spectrometer is referred to as the *object cube*.

This project primarily concerns imaging spectrometry in the mid-wave infrared (MWIR) spectral region. Mid-wave refers to the atmospheric window that exists at wavelengths between  $3.0 \mu\text{m}$  and  $5.0 \mu\text{m}$ . Outside this passband (with the exception of tightly controlled laboratory conditions or in vacuum) a short path through the atmosphere is completely opaque.

The Computed-Tomography Imaging Spectrometer (CTIS) employs a very simple optical system in order to measure the object cube *without any scanning*. The data is not measured directly, but in a manner that requires complicated post-processing to extract an estimate of the object's spectral radiance. Therefore, in contrast to the imaging spectrometers described above, the CTIS is a *snapshot instrument*.

The target application of the CTIS is a spatially non-localized or spatially complex, dynamic event which contains some useful amount of thermal or chemical structure. The application of a standard scanning spectrometer to such targets could either miss the event or return data corrupted by temporal artifacts.

The visible-wavelength CTIS has been applied in the field to imaging of missiles in flight. Furthering this application, the impact of missiles or other projectiles presents a clear advantage for the CTIS over purely imaging system or conventional spectrometers. Knowledge of a full datacube would allow observation of the physical, thermal, and chemical evolution of the event in two dimensions. This chemical and thermal data recovery potential also extends to explosions, plumes, exhausts, or flares.

The primary undertaking for this project is a realization of the theoretical model of the CTIS as a practical, field-capable MWIR instrument. Of additional interest, is the advancement of the theory to improve the design and functionality of the spectrometer.

The CTIS requires a dispersive element called a Computer Generated Hologram (CGH). Most CGH's are designed for performance at a single wavelength, however, the CTIS disperser must function over the full spectral bandwidth of the instrument. A new algorithm for design of the holographic disperser component of the CTIS has been introduced. The process permits optimization of the CGH at one or more wavelengths.<sup>1</sup>

The end result of this work is a third-generation MWIR spectrometer that operates from  $3.0\text{ }\mu\text{m}$  to  $5.0\text{ }\mu\text{m}$  and reconstructs a  $46\times 46\times 21$  voxel object cube, or  $0.1\text{ }\mu\text{m}$  spectral sampling. The field of view (FOV) of the spectrometer is variable since the objective lens may be exchanged.

### ***Summary of the Most Important Results***

#### **MWIR CTIS Instrument**

The computed tomography imaging spectrometer consists of three optical-element groups: an objective lens, a collimating lens, and a re-imaging lens (Figure 1). The Computer Generated Hologram (CGH) disperser is located in collimated space between the collimator lens and the re-imaging lens. The large-format focal plane array (FPA) is conjugate to the field stop.

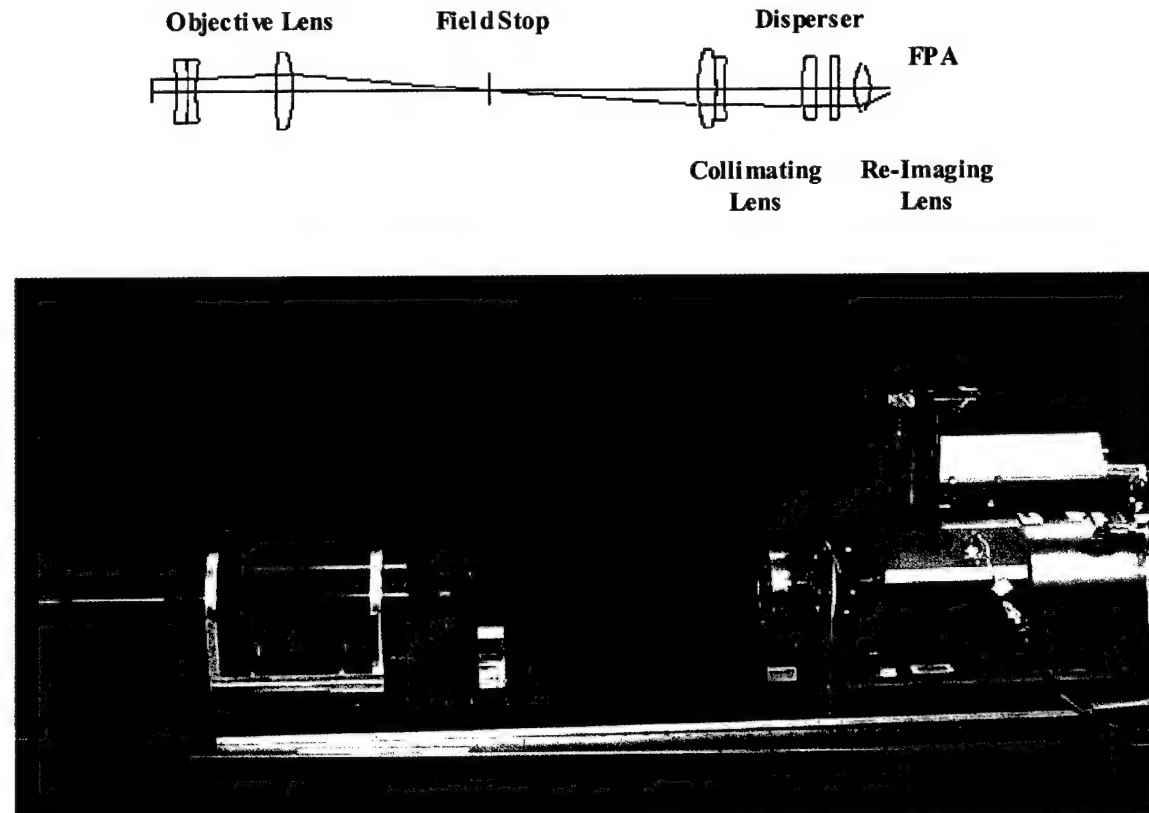


**Figure 1.** Top: Optical schematic of the CTIS including the chief ray; Bottom: MWIR CTIS instrument.

Without a CGH, the optical system images the field stop at small magnification onto the focal plane array, so that only a small portion of the FPA is dedicated to spatial resolution. The introduction of the CGH causes light to be dispersed into many additional images on the FPA. The particular design of the CTIS CGH forms a square array of equi-spaced *diffraction orders*. An example MWIR CTIS image of a monochromatic, point object is shown in Figure 2(a) (in negative contrast).

Each diffraction order is subject to dispersion (with the exception of the center order), which causes them to exhibit a linear blur. The dispersion blur for a particular order is oriented along the same direction as the diffraction. This blur can be observed in Figure 2(b), an image of a uniform, warm source.

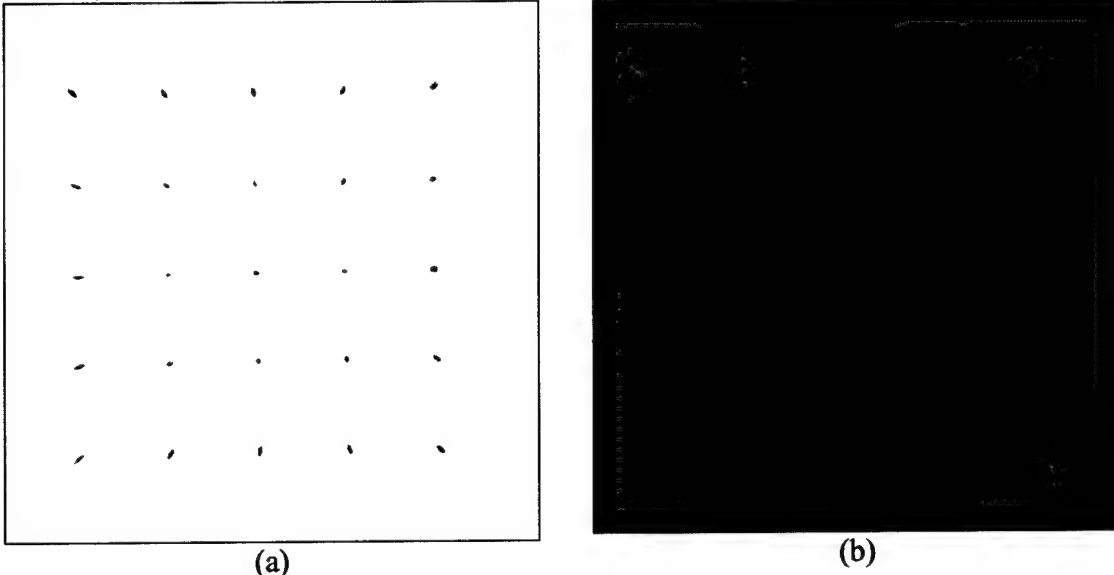
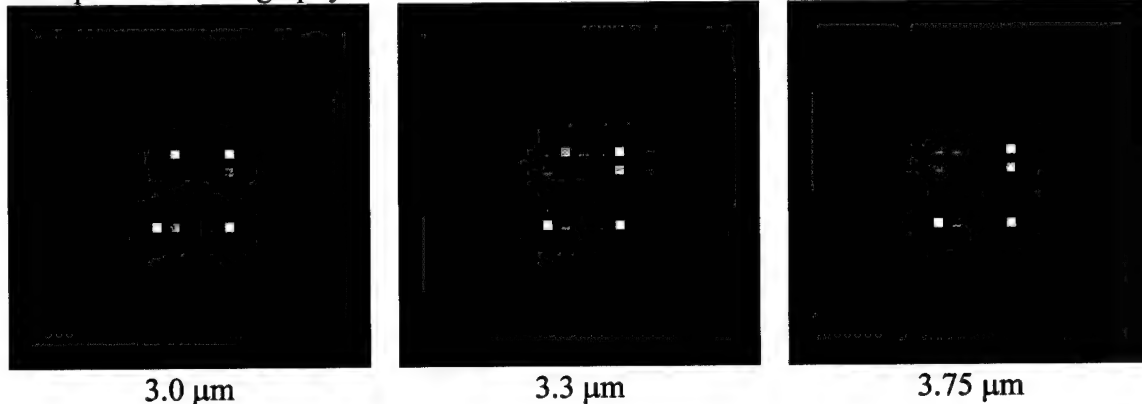


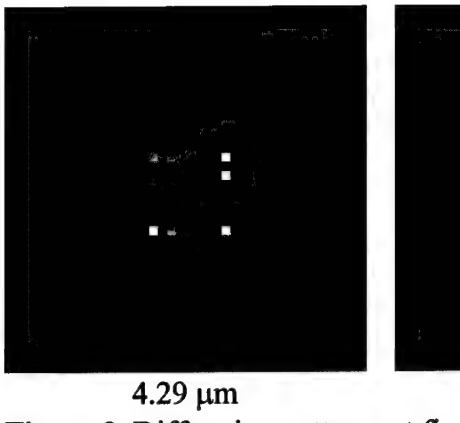
**Figure 2.** MWIR CTIS images.

The MWIR CTIS, shown in Figure 1, uses a 512 x 512 pixel InSb array with 25 $\mu$ m pitch operating at 60 frames per second with variable integration time. The 5 mm square field stop maps to an 84x84 pixel area on the focal plane array. The MWIR CTIS includes a CGH disperser designed for uniform irradiance into 5x5 orders on the 512x512 InSb array. The system uses a 100 mm re-imaging lens and a 500 mm collimating lens.

#### CGH Disperser

The CGH is designed to produce uniform peak irradiance into each of the 5x5 orders on the focal plane of the CTIS. The peak irradiance decreases with increasing dispersion, the higher orders are given higher efficiency to maintain uniform irradiance. The goal diffraction efficiency as a function of wavelength is uniform in each order. The results of this design are shown in Figure 3. The design has been discretized to 16 equally spaced levels for fabrication in GaAs using multiple-mask lithography.





diffraction efficiency: 70%

PV depth ( $3.75 \mu\text{m}$ ):  $3.40\pi$ .

**Figure 3.** Diffraction patterns at five wavelengths for the same SVD-optimized  $5 \times 5$  uniform-irradiance CGH.

The uniform-irradiance design detailed in Figure 3 was fabricated at Sandia National Laboratories. The surface profile repeats every  $190 \mu\text{m}$ . A WYKO NT2000<sup>2</sup> depth measurement of the fabricated CGH is shown in Figure 4.

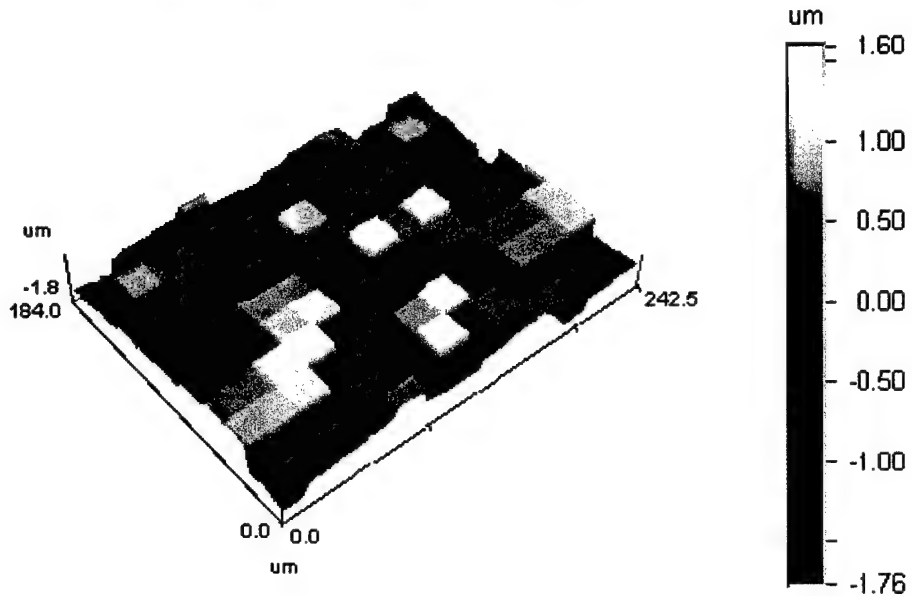
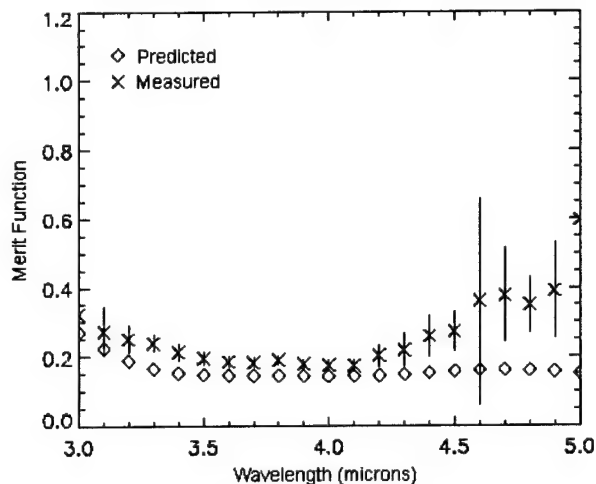


**Figure 4.** WYKO NT2000 depth measurement of the fabricated uniform-irradiance CGH.

CTIS images of monochromatic sources can be used to estimate the similarity between the expected and measured CGH performance.<sup>3</sup> A merit function is calculated for each wavelength since wavelength-to-wavelength comparisons are not possible (orders outside the center  $5 \times 5$  fall outside of the FPA). The merit function is the standard deviation of the normalized center  $5 \times 5$  diffraction efficiencies. Normalization consists of dividing the irradiance into each order by its goal efficiency, then setting the average to unity. A plot of the expected and measured merit functions is shown in Figure 5. Error bars indicate the contribution of estimation error from the use of noisy calibration images. Discrepancies between the predicted and measured merit

function result from fabrication error and inaccuracies in the Fraunhofer diffraction model used in the design process.

**Figure 5.** Calculated vs. measured merit function for the uniform-irradiance CGH.



### Reconstruction Algorithms

Reconstruction employs two primary iterative algorithms, the Multiplicative Algebraic Reconstruction Technique (MART) and Expectation Maximization (EM). Each iteration of the reconstruction algorithms takes approximately five seconds for  $46 \times 46 \times 21$  ( $x, y, \lambda$ ) sampling.<sup>4</sup>

A procedure to improve the results of the reconstruction using *a priori* information about measurement confidence is often used between iterations of MART or EM. The spectral principal components may be calculated from a partially reconstructed datacube. Subsequent iterations are constrained by the principal components to reduce reconstruction error and artifacts.

### Reconstruction Results

Two targets have been examined to provide a broad study of the instrument's reconstruction capabilities. The first target examined consists of a warm, flat-black panel partially obscured by a broadband (3.4 - 3.9 FWHM) pass filter. The raw image is shown in Figure 6. The reconstruction shown in Figure 7 was calculated using nine iterations of EM with the constraints applied for the first eight iterations. The filter wheel is the large black object in the lower part of the spectral images. The broadband filter is located in the lower right aperture of the filter wheel, as shown in the contrast-enhanced copy of the 3.7  $\mu\text{m}$  spectral image (Figure 7, upper right).

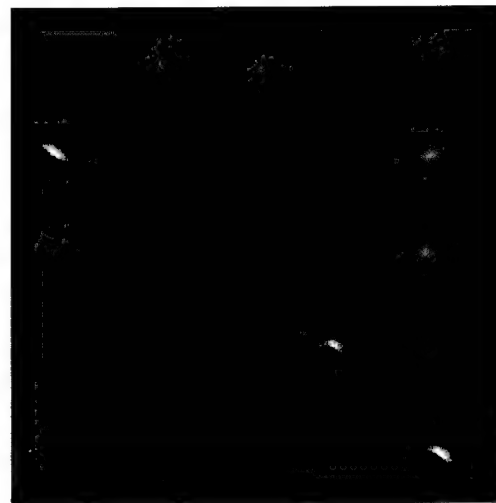


**Figure 6.** Raw image of the broadband filter target.

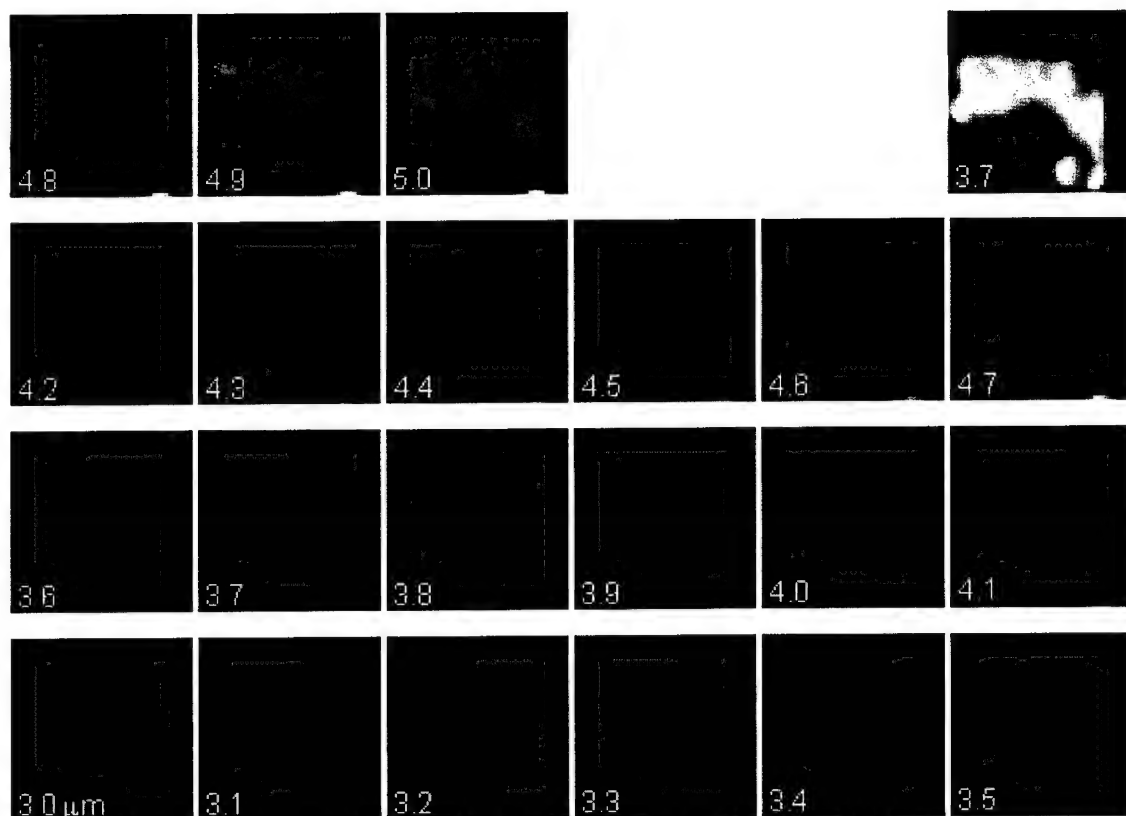


**Figure 7.** Spectral images from a reconstruction of the broadband filter target.

The second target of interest demonstrates the temporal resolution of the CTIS. The target consists of a burning match viewed through an attenuating filter. After burning for several seconds, the spectral emission of the scene contains two different spectral species, the first from the smoldering match and the second from the emission from hot CO<sub>2</sub> gas.

The spectral images are shown in Figure 8. The flame is brightest in the  $4.4\text{ }\mu\text{m}$  spectral image while the smoldering match appears brighter in the  $4.8\text{ }\mu\text{m}$  spectral image. The spectra from points near the center of the flame and match are shown in Figure 9(a) and (b), respectively.

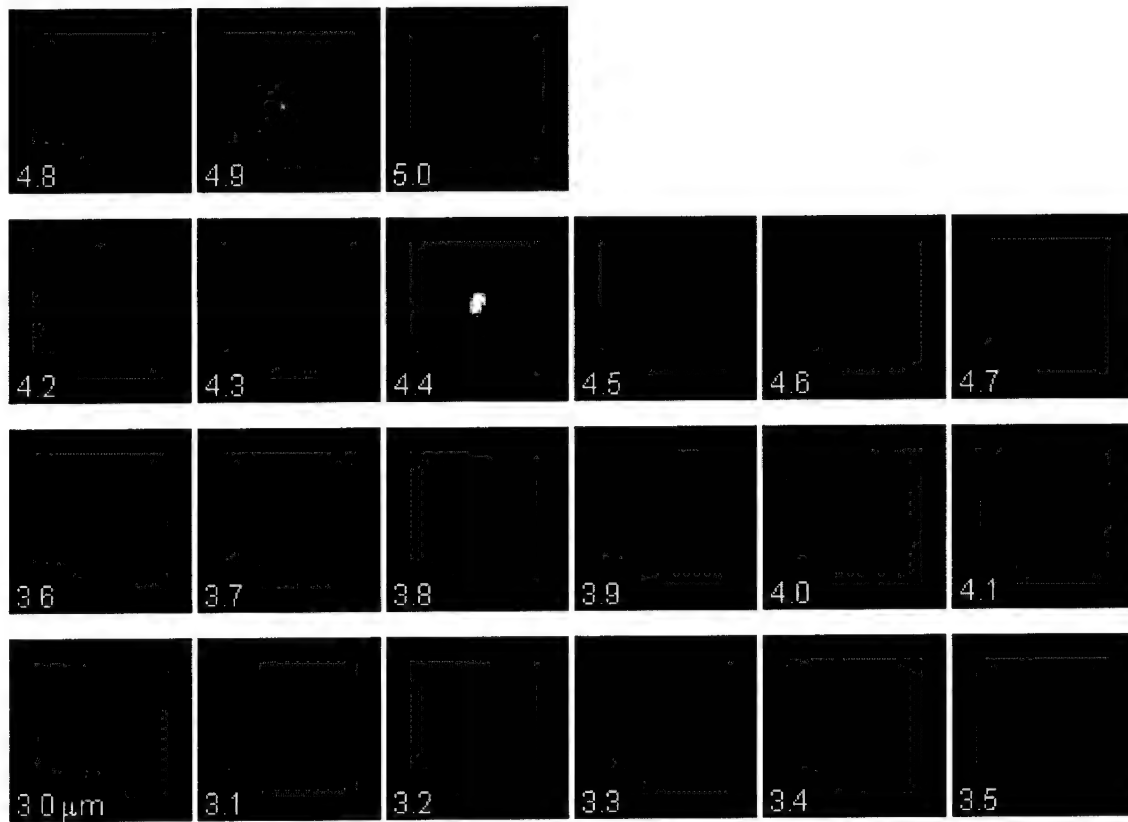


**Figure 8.** Spectral images from the reconstruction of the burning match target.

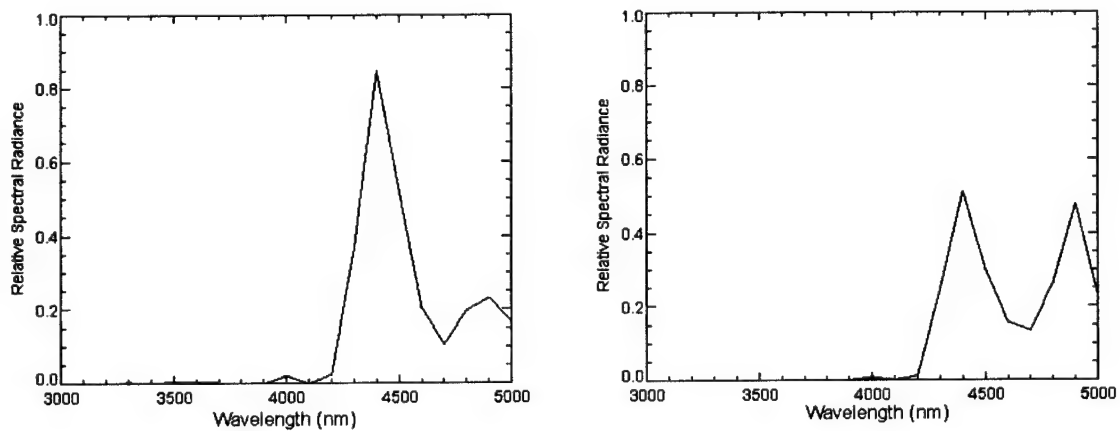


**Figure 9.** Spectra from selected resels in the burning match datacube.

### ***List of Publications and Technical Reports***

1. Curtis E. Volin, "Portable Snapshot Infrared Imaging Spectrometer," Ph.D. Dissertation, University of Arizona (2000).
2. C. E. Volin, J. P. Garcia, M. R. Descour, E. L. Dereniak, D. T. Sass, C. G. Simi, "Demonstration of a MWIR high-speed nonscanning imaging spectrometer," in Automatic Target Recognition IX, Firooz A. Sadjadi; Ed., Proc. SPIE 3718, 480-489 (Aug 1999).
3. C. E. Volin, J. P. Garcia, E. L. Dereniak, M. R. Descour, D. T. Sass, C. G. Simi, "MWIR computed-tomography imaging spectrometer: calibration and imaging experiments," in Imaging Spectrometry V, Michael R. Descour; Sylvia S. Shen; Eds., Proc. SPIE 3753, 192-202 (Oct 1999).
4. C. E. Volin, J. P. Garcia, D. S. Sabatke, M. R. Descour, T. K. Hamilton, "MWIR Snapshot Imaging Spectrometer: Calibration and Imaging Experiments," ( March 2000).

### ***Scientific Personnel***

#### **Graduate Students partially supported by this grant**

Raviv Levy, Research Assistant

Daniel S. Simon (MS awarded, 1998), Research Assistant

Mark R. Willer, Research Assistant

William R. Davidson (MS awarded, 1999)

#### **Research Associate**

Curtis E. Volin, (Ph.D. awarded, December 2000)

#### **Research Scientist**

John P. Garcia

#### **Professor**

Michael R. Descour

### ***Report of Inventions***

"MWIR Imaging Spectrometer" (patent disclosure filed, 2000)

"Multichromatic Computer Generated Hologram" (invention disclosure December 1998)

## ***Bibliography***

---

1. Curtis E. Volin, "Portable Snapshot Infrared Imaging Spectrometer," Ph.D. Dissertation, Chapter 3, University of Arizona (2000).
2. Veeco Instruments, Corp., Tucson, AZ.
3. Volin, Chapter 6.
4. Volin, Chapter 4.

## NUMERICAL MODELING OF NONLINEAR OPTICAL FREQUENCY CONVERSION

Robert Eckardt

### *Statement of the Problem Studied*

Numerical modeling of nonlinear frequency conversion processes such as harmonic generation, sum and difference frequency generation, and parametric amplification are necessary in the analysis of experimental results and engineering design of practical systems. The increasing complexity of the systems being analyzed requires numerical techniques greater capability than the more simple analytical models. The numerical model developed in this program has been used for the analysis of harmonic generation in mixed crystals with non-uniform index of refraction, sum-frequency generation for applications in sodium guide star lasers, and infrared harmonic generation in materials with large levels of absorption. The calculation includes the effects of diffraction, birefringent walkoff, nonlinear frequency conversion with pump depletion and back conversion, and different levels of absorption at the various wavelengths involved. Calculations of phase-matching parameters and beam propagation are being combined with the nonlinear conversion calculation to provide guidance in the selection of parameters to optimize the nonlinear optical frequency conversion process. The development of this numerical model is continuing. Thermal effects of lensing and stress birefringence will be added in a new project. Through technology transfer, the results of the calculations have been provided to four companies: Lite Cycles, Cleveland Crystals, Sanders, and DeMaria Electro-Optical Systems. The numerical model is described in the next section. The application of the model to infrared harmonic generation, sum frequency generation for the generation of guide-star radiation, and infrared difference frequency generation is described in following.

### *Summary of the Most Important Results*

#### **The Numerical Model**

At present this model includes the effects of nonlinear conversion with depletion and back conversion, diffraction, birefringent walkoff, and absorption. The calculations are intended to be used for nanosecond duration pulses and do not include group velocity dispersion effects. Nonlinear optical conversion is followed through the pulse duration to give calculations of total conversion and spatial distributions at different times.

A split-step technique is used in the calculation. The nonlinear crystal is divided into a number of length increments. Diffraction and walkoff are calculated from the center of one increment to the center of the next increment using two-dimensional fast Fourier transform techniques. The nonlinear interaction and absorption effects are calculated over each length increment using a second order Runge-Kutta method applied to each transverse element in the distribution. A number of tests were used to verify the accuracy of the model. These tests included propagation of top-hat and Gaussian beams and comparison to analytical solutions, and reproducing phase-matching tuning curves obtained for low levels of conversion using the results of Boyd and Kleinman. Convergence of the numerical solution is checked by increasing the number of increments until there is no significant change in the calculated beam distributions and

conversion efficiency. Satisfactory results were usually obtained with 32x32 transverse sampling points and 16 longitudinal increments in calculations performed to this time. In most of the calculations we perform now, 64x64 transverse sampling points with 32 length increments are used. Calculations with up to 256x256 transverse sampling points are possible with this calculation but become time consuming on the computers being used.

### Harmonic Generation in a Mixed Crystal

Phase matching is typically achieved in a nonlinear crystal by balancing the effects of dispersion with birefringence. The nonlinear infrared crystal  $\text{AgGaSe}_2$  is a negative uniaxial birefringent crystal, that is, the extraordinary index is less than the ordinary index. Phase matching is achieved by using an ordinary fundamental and an extraordinary harmonic. This material has a nonlinear tensor component that couples the harmonic and fundamental of different polarizations. The birefringence is tuned by changing the angle of propagation in the crystal to provide exactly the birefringence necessary to balance dispersion. If the phase-matching direction is not along a principal crystal axis there will be birefringent walkoff. In  $\text{AgGaSe}_2$  the phase-matching angle for second-harmonic generation of 10.6- $\mu\text{m}$   $\text{CO}_2$  laser radiation is  $55.3^\circ$  and the walkoff angle is  $0.7^\circ$ . The phase-matching angle for second-harmonic generation of 9.27- $\mu\text{m}$   $\text{CO}_2$  laser radiation changes to  $47.6^\circ$  and the walkoff angle remains  $0.7^\circ$ . The walkoff angle limits how tightly the beams can be focused, and therefore, reduces the intensity which can be achieved with the available power. The nonlinear harmonic conversion efficiency is reduced when intensity is reduced.

It is possible to grow a mixed crystal of  $\text{AgGa}_{(1-x)}\text{In}_x\text{Se}_2$  to control birefringence and achieve phase matching at  $90^\circ$  to the optic axis with no walkoff. However, the molar indium concentration  $x$  cannot be precisely held at this value during the growth process. The question addressed with numerical modeling was how does the variation of  $x$  over the length of the crystal change the second harmonic conversion. The dispersion of both  $\text{AgGaSe}_2$  and  $\text{AgInSe}_2$  are known, and the dispersion of the mixed crystal can be interpolated using the indium molar concentration. Fig. 1 shows calculated conversion efficiencies for mixed crystals of linearly varying composition. Tolerances for compositional variation can be obtained from such calculations. Numerical modeling allows investigations that would be very difficult experimentally. This is the case for the calculations of Fig. 1 where it would be impossible to experimentally obtain a large number of crystals from different positions in a single boule of varying composition.

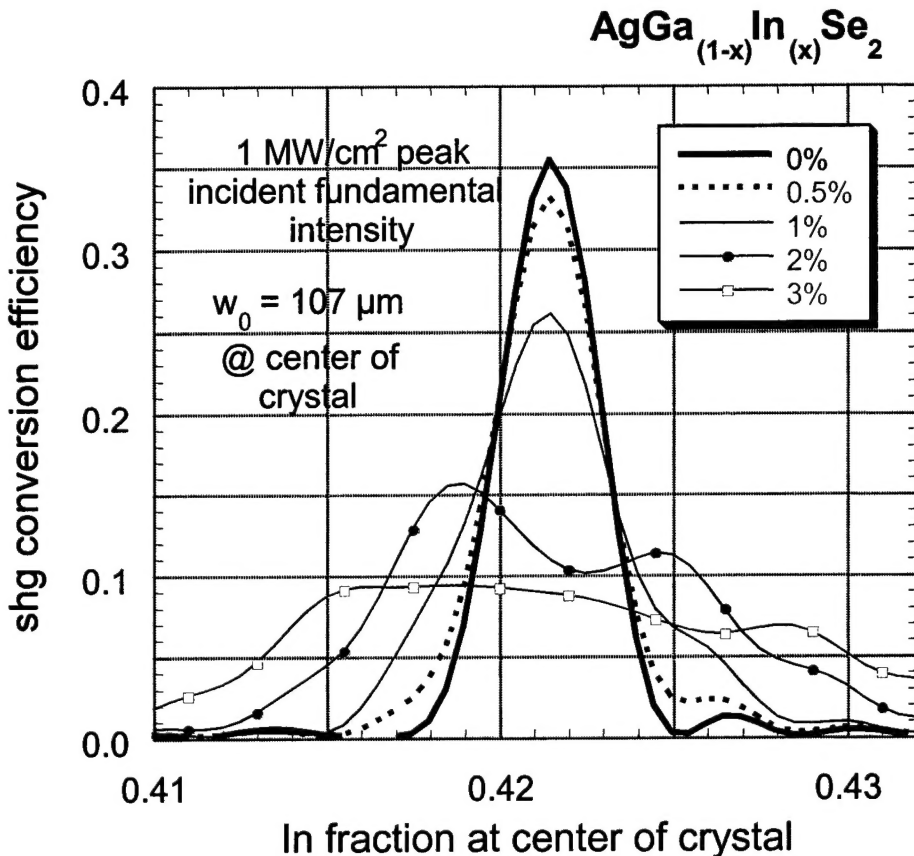


*Fig. 1. Calculations of harmonic generation with optimum focusing of a 9.27- $\mu\text{m}$  fundamental beam in the mixed crystal AgGa<sub>(1-x)</sub>In<sub>x</sub>Se<sub>2</sub>. The curve for uniform composition is labeled 0%. The other curves assume a linear increase of In fraction from the input to exit surfaces of the amount shown (e.g. at 0.42 center composition the curve for 2% uses 0.41 at the input and 0.43 at the exit). Calculations are for a 0.4-cm-long crystal. This is an instantaneous power calculation spatially summed over the beam.*

### Sum Frequency Generation of Sodium Guide-Star Radiation

There is a need for high-optical-quality laser beams at 589-nm for adaptive optics astronomy. The guide star beam is focused on a layer of the atmosphere at an altitude of 90 km that contains sodium. The size of the beam focus at this altitude needs to be about 30 cm in diameter. There are stringent tolerances of 1.0 GHz bandwidth to match the sodium absorption at 589.2 nm. An average power of 10 W is also necessary. It has been very difficult and expensive to satisfy all of these requirements in a laser system to generate the guide star radiation. One of the most promising approaches is sum-frequency generation of 1319-nm Nd:YAG laser radiation and 1064-nm Nd:YAG laser radiation. The laser systems are synchronously mode locked to produce trains of 750-picosecond duration micro pulses in a longer macro pulse of perhaps 150  $\mu\text{s}$  duration.

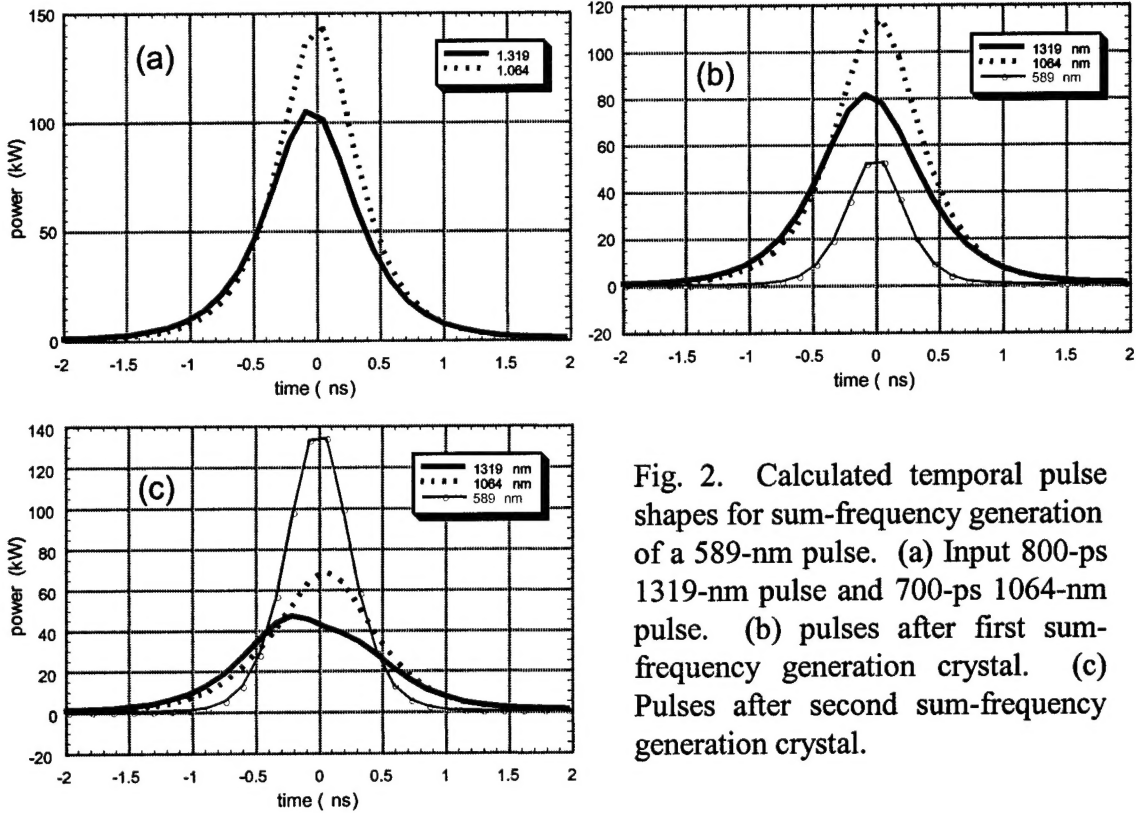
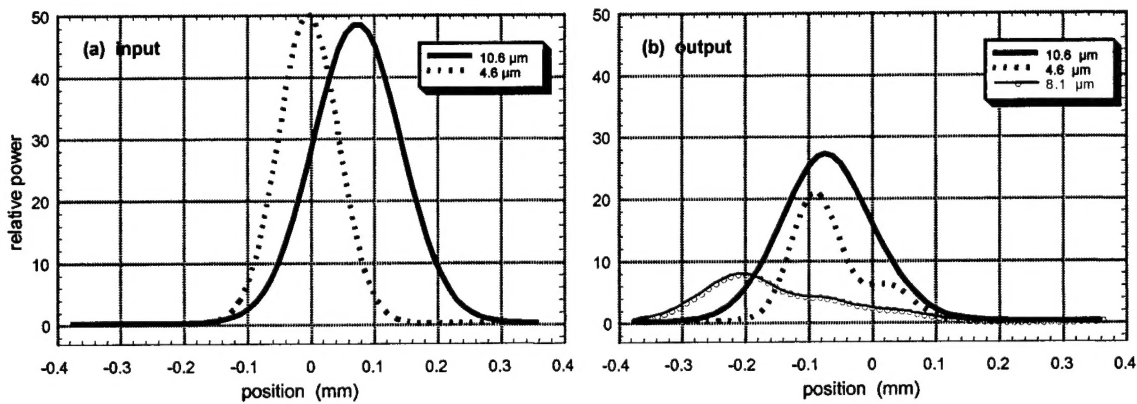


Fig. 2. Calculated temporal pulse shapes for sum-frequency generation of a 589-nm pulse. (a) Input 800-ps 1319-nm pulse and 700-ps 1064-nm pulse. (b) pulses after first sum-frequency generation crystal. (c) Pulses after second sum-frequency generation crystal.

This pulse format provides the required bandwidth and duration to avoid saturation of the sodium absorption and provides peak powers at which the sum-frequency generation becomes feasible.

Figure 2 illustrates the temporal pulse shapes of a calculation of sum-frequency generation. The calculation used incident micro pulses of 800-picosecond duration and 0.1-mJ energy at 1319 nm and 700-picosecond duration and 0.12-mJ energy at 1064 nm. The pulses were assumed to have diffraction limited Gaussian transverse distributions and hyperbolic secant shapes in time. In this calculation, it was also assumed that the pulses were displaced 50 picosecond in time. A spatial displacement was not used but would also be possible since the beams are defined on a square array of sampling points. The beams were focused into a 2-cm-long  $\text{LiB}_3\text{O}_5$  nonlinear crystal with waists of 30  $\mu\text{m}$  and 27  $\mu\text{m}$  for the 1319-nm and 1064-nm beams respectively. Sum frequency generation was increased by relay focusing into a second 2-cm-long  $\text{LiB}_3\text{O}_5$  crystal with appropriate phase retardation of the three beams. This type of calculation is useful for engineering design and in the selection of nonlinear materials and establishing pump beam requirements.



*Fig. 3. Calculated spatial distributions for difference frequency generation of 4.6- $\mu\text{m}$  radiation and 10.6- $\mu\text{m}$  radiation to generate 8.1- $\mu\text{m}$  radiation. The nonlinear material  $\text{ZnGeP}_2$  has positive birefringence. The 10.6- $\mu\text{m}$  and generated 8.1- $\mu\text{m}$  radiation have extraordinary polarization, and therefore experience birefringent walkoff in the crystal. The 10.6- $\mu\text{m}$  beam is to the right of the ordinary 4.6- $\mu\text{m}$  beam at the input to the crystal (a). The extraordinary beams walkoff to the left at the output (b). The material  $\text{ZnGeP}_2$  has absorption of about  $0.5 \text{ cm}^{-1}$  at 10.6  $\mu\text{m}$  and  $0.04 \text{ cm}^{-1}$  at 8.1  $\mu\text{m}$  causing significant power loss in the 1.5-cm-long crystal.*

### Difference-Frequency Generation in the Infrared

There are no convenient lasers that provide high-power radiation in the spectral region from 7.5  $\mu\text{m}$  to 9  $\mu\text{m}$  in the infrared, and nonlinear frequency conversion of the output of established laser systems is a viable candidate. Waveguide  $\text{CO}_2$  lasers using rf excitation operate efficiently at a number of wavelengths near 10  $\mu\text{m}$ . These lasers can be pulsed by cavity dumping techniques. A repetitively pulsed  $\text{CO}_2$  laser operating at 9.2  $\mu\text{m}$  has been efficiently converted to 4.6  $\mu\text{m}$  by second harmonic generation. The 7.5 – 9- $\mu\text{m}$  spectral region can be reached by difference frequency generation of the 4.6- $\mu\text{m}$  radiation and 10.6- $\mu\text{m}$  radiation. There are a few nonlinear materials that are candidates for this application, but each material has individual limitations.  $\text{AgGaSe}_2$  has good transmission with absorption less than  $0.02 \text{ cm}^{-1}$  for all the wavelengths considered here, that is between 4.6 and 10.6  $\mu\text{m}$ . However,  $\text{AgGaSe}_2$  has relatively low nonlinear coefficient and low thermal conductivity, which leads to problems of thermal lensing and thermally induced changes in birefringence.  $\text{ZnGeP}_2$  has a higher nonlinearity and excellent thermal and mechanical properties, but it has a large absorption at 10.6  $\mu\text{m}$ .  $\text{CdGeAs}_2$  is a nonlinear material that is becoming available again. It has very high nonlinearity, but also has problems with absorption. The high nonlinearity allows use for shorter lengths, which will alleviate the absorption problems. The shorter lengths will also allow tighter focusing to increase conversion, but problems of optical damage to the material increase at higher intensity. Numerical modeling is useful to evaluate the use of these materials.

Figure 3 illustrates a calculation of sum-frequency generation in ZnGeP<sub>2</sub> for generation of 8.1- $\mu\text{m}$  radiation. Here the transverse distributions of the beams are shown. The effects of the birefringent walkoff and the absorption in the crystal are evident. The phase of the beams can also be retrieved in this calculation. With knowledge of intensity distribution and phase distribution, it is possible to evaluate the optical quality of the generated beams.

### **Conclusion**

This portion of the JSOP program supported the development of a numerical model for nonlinear frequency conversion. The model included nonlinear conversion with depletion and back conversion, absorption, diffraction, and birefringent walkoff. The performance of this numerical model has been demonstrated with calculations that show total conversion efficiency, temporal pulse shapes, and transverse beam distribution in applications of the model to actual problems. This model is a tool for analysis of experimental investigations and engineering design. It has been used in technology transfer with companies outside the University. Results of harmonic generation in mixed crystals were first supplied to Cleveland Crystals on a consulting basis for a phase-I SBIR. Later the mixed crystal analysis was extended and results were supplied to Sanders Associates for inclusion in a research proposal. The calculations for sum-frequency generation were supplied to Lite Cycles for use in a proposal on a guide star laser system. The infrared difference frequency calculations are being used in program that is funded by DeMaria Electro-Optical Systems through a subcontract to a phase-II SBIR program. This numerical model for nonlinear frequency conversion is being used in our own research and in a collaborative effort with Steward Observatory. The development of the model is also continuing in other programs.

### ***List of Manuscripts and Technical Papers***

None

### ***Scientific Personnel***

#### **Research Professor**

Robert Eckardt

### ***Report of Inventions***

None